

Hadron Calorimetric Detectors for the future High Energy Physics Experiments

V. Mikhaylov^{1,2,3}, V. Kushpil¹, F. Guber⁴, A. Kugler¹, S. Kushpil¹, V.P. Ladygin⁵, A. Ivashkin⁴,
I. Selyuzhenkov⁶, O. Svoboda¹, S. Seddiki⁶, P. Tlustý¹

¹NPI ASCR (Czech Republic); ²CTU (Czech Republic); ³TPU (Russia); ⁴INR of RAS (Russia); ⁵JINR (Russia); ⁶GSI (Germany)

EPS-HEP 22-29 July 2015, Vienna, Austria

Hadron Calorimeter: Outline

Primary task: measurement of the total energy of particles

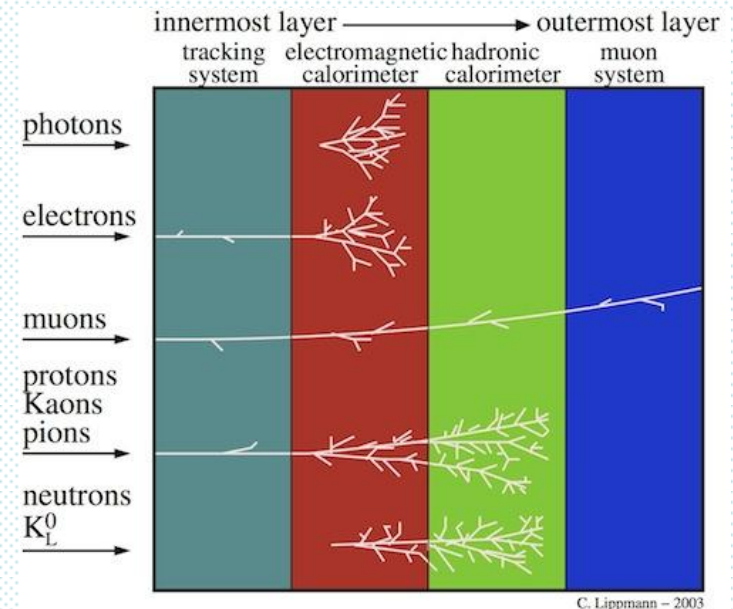
- Energy -> electrical signal (ionization charge)
-> light signal (scintillators, Cherenkov light)
- Cascades of secondary particles:
 - Electromagnetic fraction
 - Hadronic fraction

e/h ratio $\neq 1$ -> compensation required

EM fraction increases with energy -> non-linearity

OUTLINE:

- 2-4 HCAL: Types & Observables
- 5-8 HCAL: Existing designs
- 9-12 HCAL: Results on performance simulations
- 13 HCAL: Module tests
- 14-16 HCAL: Results on radiation hardness
- 17 Conclusions and Outlook



Hadron Calorimeter: Type

- Calorimeter types:

Homogeneous Calorimeters

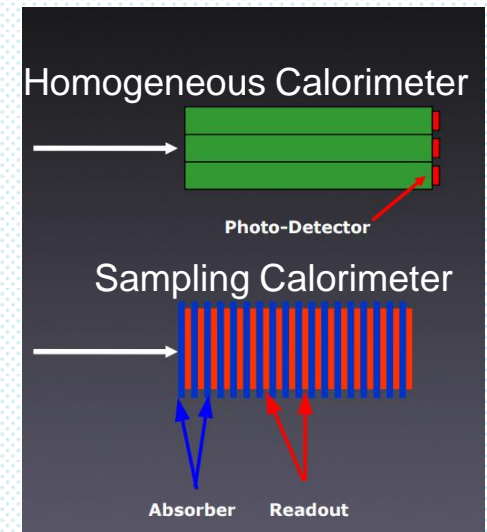
- Good resolution
- No direct longitudinal shower information
- Scintillating crystals are expensive
- Very non-linear for hadrons

Sampling Calorimeters (the most popular for hadrons)

- High granularity both lateral and longitudinal
- Two ingredients: active (readout) & passive (absorber)
- Types: Sandwich/Spagetti/...

- **Readout:**

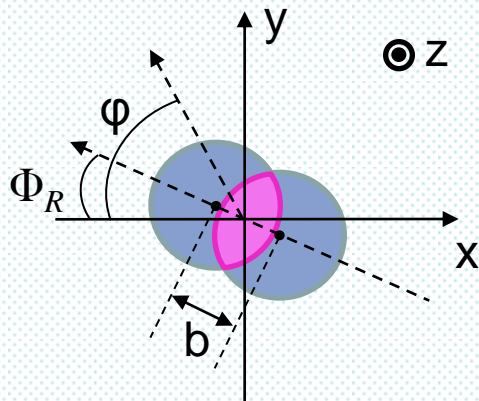
- Light (Scintillators + Photomultipliers / Avalanche Photo-Diodes)
 - Charge (Silicon, Gas detectors, Liquid noble gases)
- Analog or digital



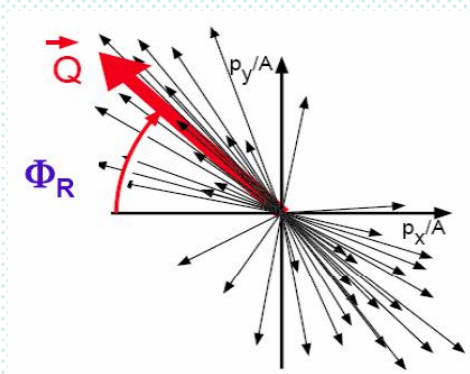
Hadron Calorimeter: Observables

Hadron Calorimeter measures number of projectile nucleons and fragments and therefore initial event geometry.

Collision centrality



Reaction plane orientation



Particle flow components and fluctuations:

Directed (side) flow

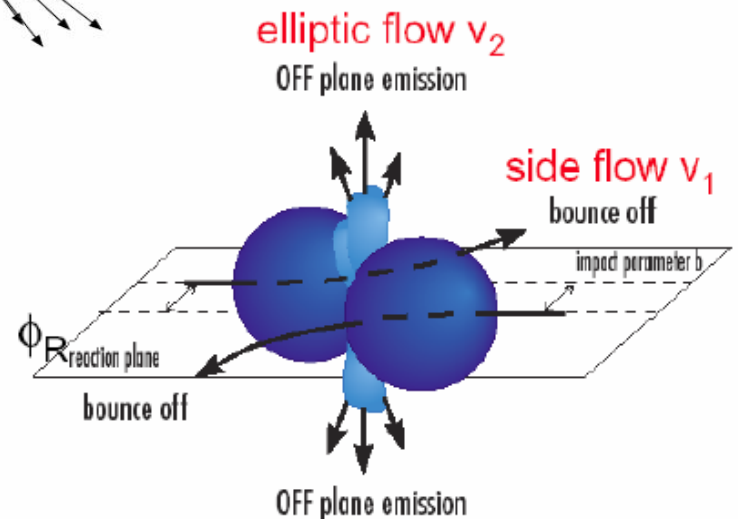
$$v_1 = \langle \cos(\varphi') \rangle$$

Elliptic flow

$$v_2 = \langle \cos(2\varphi') \rangle$$

$$\varphi' := \varphi - \Phi_R$$

$$\frac{d^3N}{p_i dp_i dy d\varphi'} \propto (1 + 2v_1 \cos(\varphi') + 2v_2 \cos(2\varphi'))$$



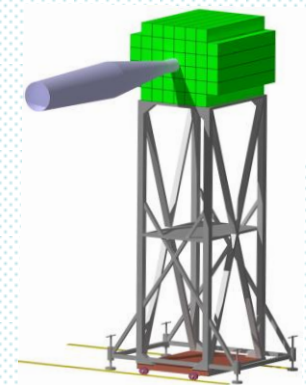
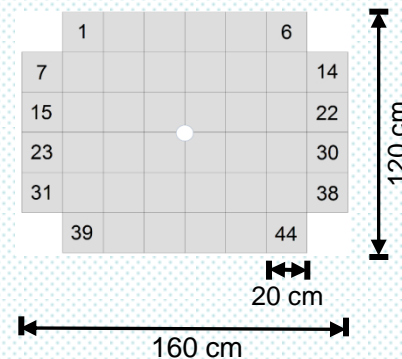
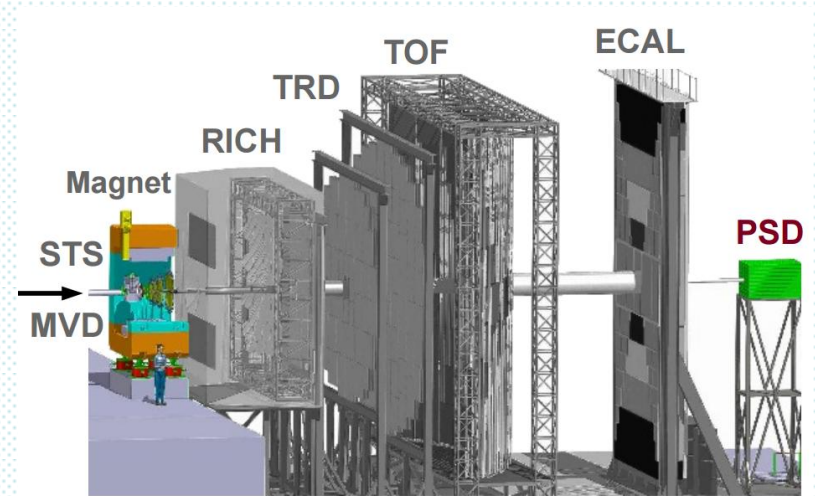
CBM Projectile Spectator Detector

Full compensating modular lead-scintillator sandwich calorimeter

Main features:

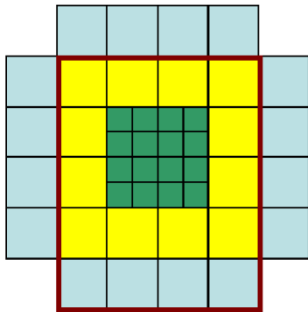
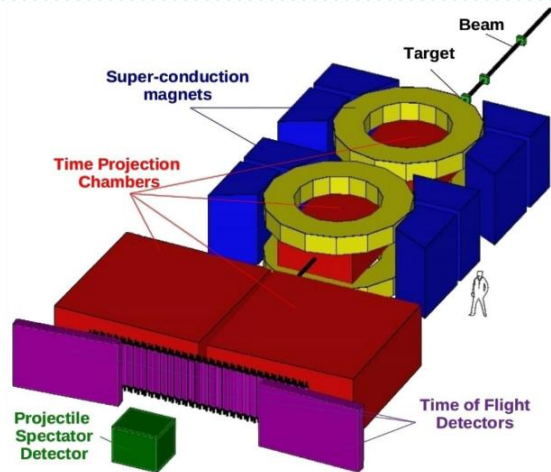
- high transverse granularity
transverse homogeneity of energy resolution, reaction plane measurements
- lead/scintillator sampling ratio 4:1 (16 mm / 4 mm), compensating calorimeter ($e/h = 1$)
high energy resolution $< 60\%/\sqrt{E(\text{GeV})}$
- longitudinal segmentation (10 sections per module)
particle identification, calibration, improved energy resolution
- light readout from each section by novel APDs
large dynamic range up to 10^4 ph.el., no nuclear counting effect
- ability to operate at high count rate and at high radiation dose

60 sandwiches in one module
 45 modules of 20 x 20 x 120 cm³
 Total weight ~ 22 tons, 8-15 m from target
 Beam hole (d = 6 cm) for intensity up to 10⁹ ions/sec
 CBM beam energy up to 35 AGeV (SIS300)



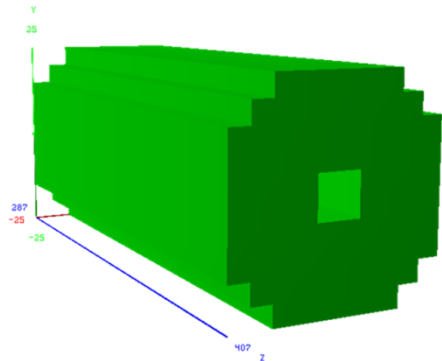
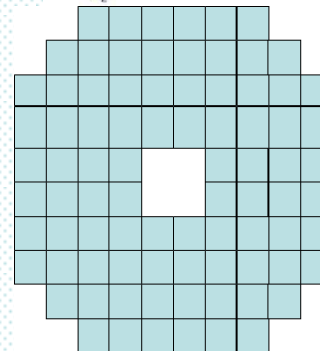
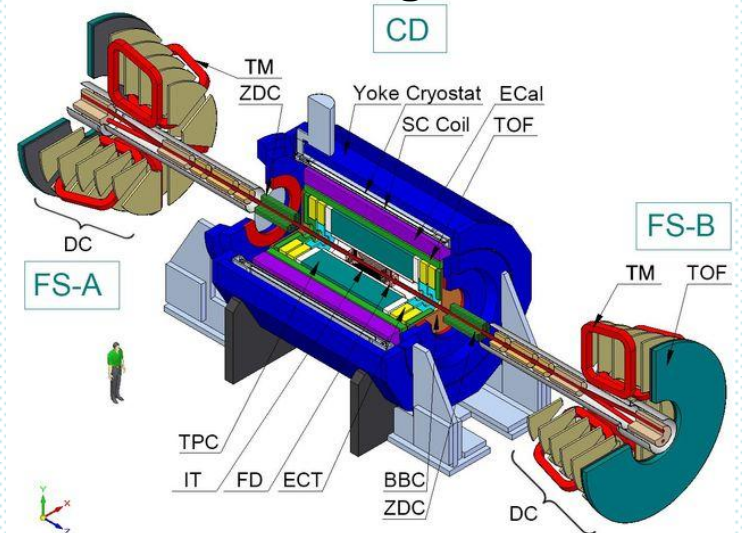
Similar Calorimeters

NA61 Projectile Spectator Detector



60 sandwiches in one module
 16 inner modules of $10 \times 10 \times 120 \text{ cm}^3$
 28 outer modules of $20 \times 20 \times 120 \text{ cm}^3$
 Total weight ~ 17 tons, 17-25 m from target
 No beam hole for intensity up to 2×10^5 ions/sec
 NA61 beam energy up to 150 AGeV

NICA MPD Zero Degree Calorimeter



60 sandwiches in one module
 16 modules of $5 \times 5 \times 120 \text{ cm}^3$
 Total weight ~ 10 tons, 28 m from collision estimate
 Beam hole ($10 \times 10 \text{ cm}$) for intensity up to 1×10^9 ions/sec
 NICA beam energy up to $\sqrt{s_{NN}} = 11 \text{ GeV}$ ($\sim E_{\text{beam}} = 63 \text{ AGeV}$)

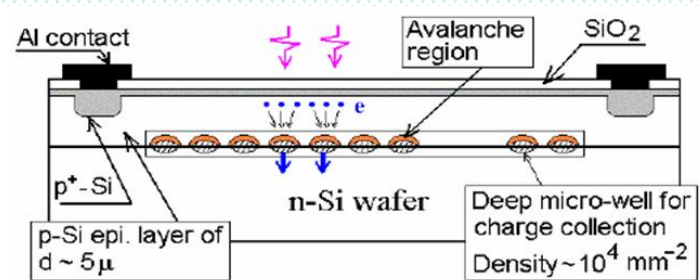
CBM PSD: Module Design

Fibers from each consecutive 6 layers are collected together via WLS-fibers and read-out by a single **Avalanche Photo-Diode (APD or SiPM)**.

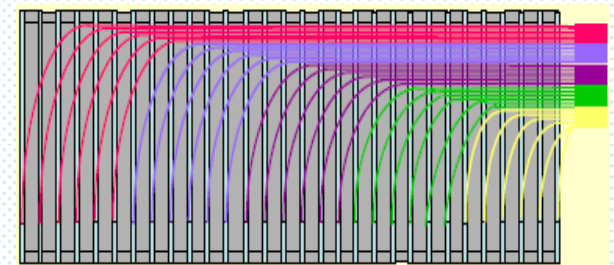
60 sandwiches in one module
10 sandwiches = 1 section, read out by 1 APD
Module of 20 x 20 x 120 cm³
Depth ~ 5.7 λ_{int}

APD properties:

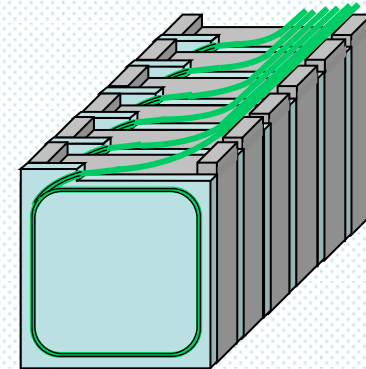
- size: 3x3 mm²
- high dynamical range: 5-15000 ph.el.
- photon detection efficiency: ~15%
- high counting rate ~ 10⁵ Hz
- requirements: radiation hardness to neutrons
~10¹³ n/cm² for CBM



APD with deep micro-wells



TOP View

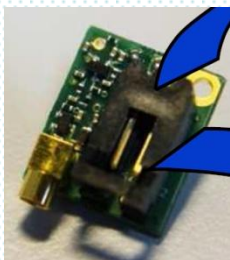


FRONT View

CBM PSD: Readout Electronics

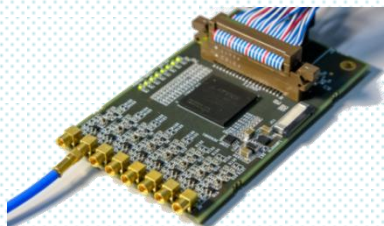
Preamplifier:

- Directly attached to photodiode
- 2 stage, optimized for high capacitance inputs
- Gain: 60 V / V
- Signal / Noise = 864:1



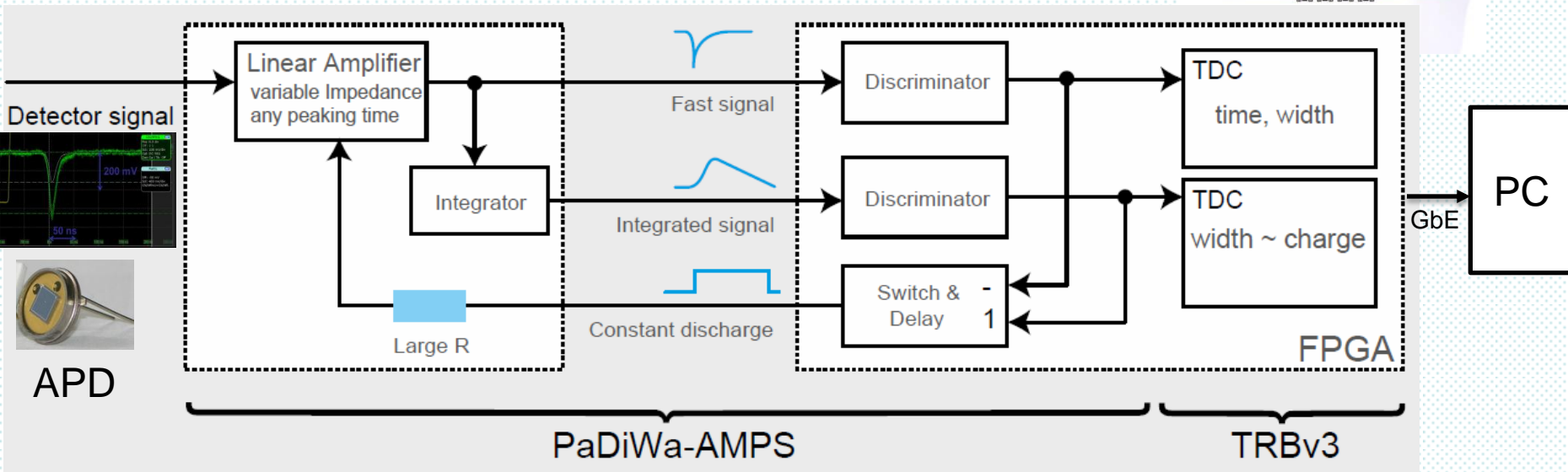
PaDiWa-AMPS:

- 8 MMCX input channels
- Time precision: < 50 ps
- Rel. charge resolution: < 0.5 %
- Dynamic range: ~250
- Compact data : max. 50 MB/s



Trigger and Readout Board:

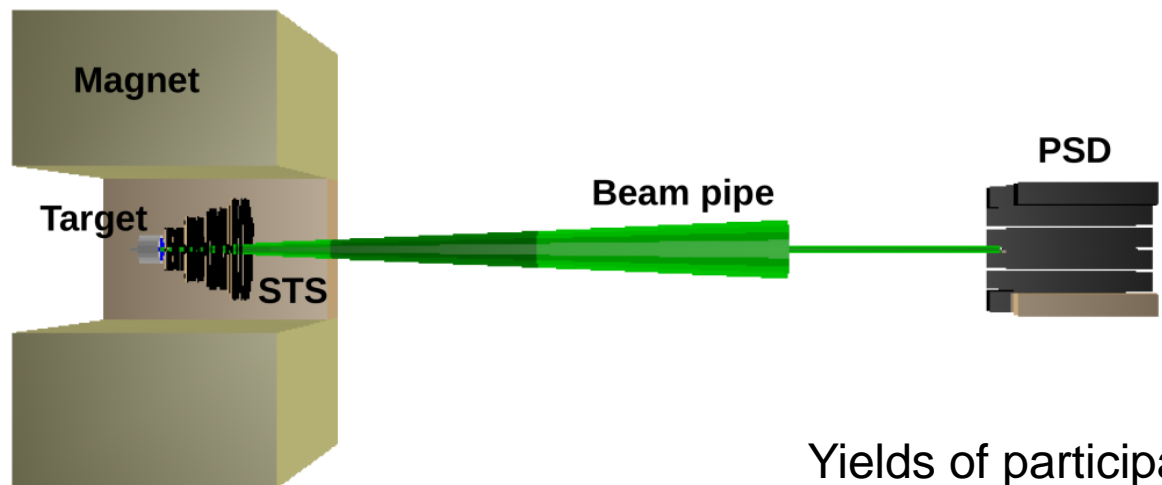
- 4 FPGAs, 260 TDC channels
- Single edge & ToT measurement
- Time precision < 20 ps
- 50 MHz hit rate per channel
- Extendable by add-ons
- Internal trigger and slow control



From poster of A.Rost at ICST in Worms, 2014

CBM PSD: Experimental and simulation results

CBM PSD: Simulation setup



PSD detector is located:

- at 8 m from target for $E_{\text{beam}} = 2\text{-}8$ AGeV
- at 15 m from target for $E_{\text{beam}} = 30$ AGeV

Simulation:

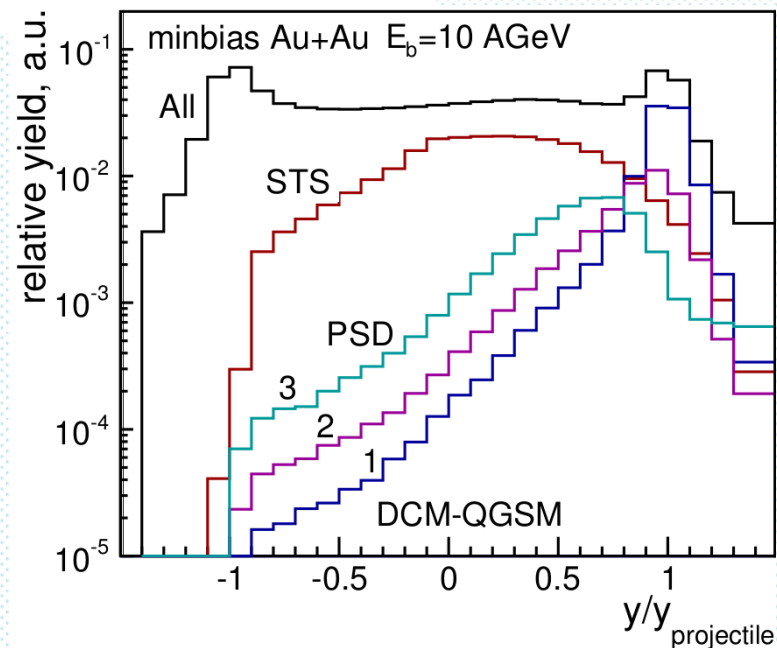
4 event generators:

UrQMD, HSD, DCM-QGSM, LA-QGSM

+ *CBMROOT* for analysis

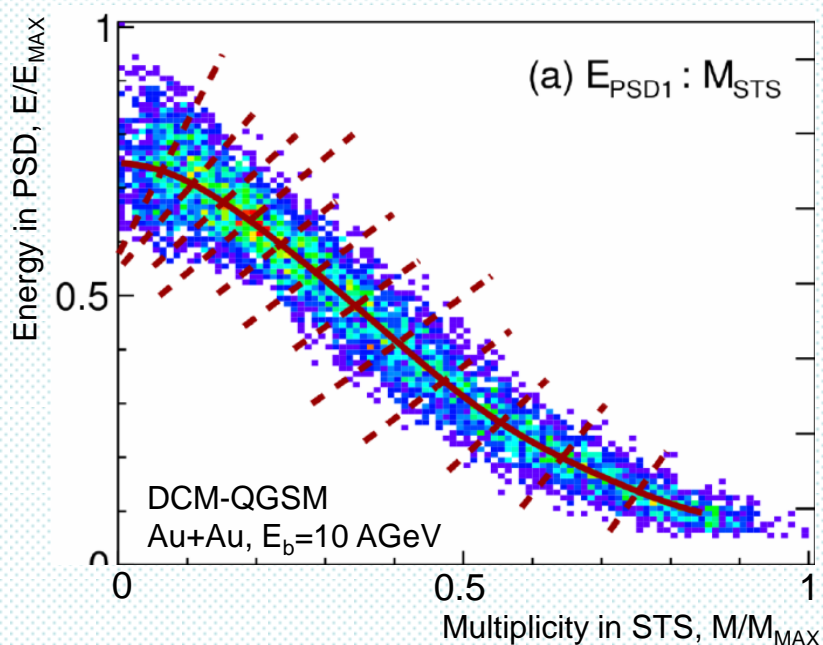
+ *GEANT4* for particles transport
through the detector geometry

Yields of participants & spectators



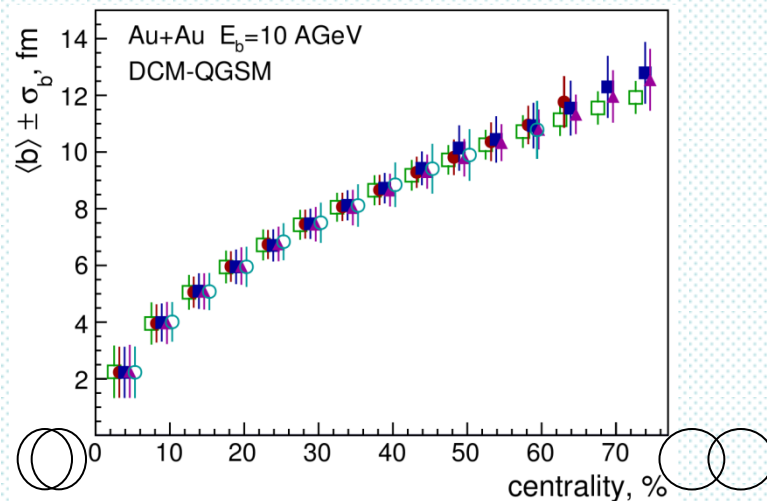
CBM PSD: Centrality performance

Centrality determination by correlation between energy deposited in PSD & STS track multiplicity

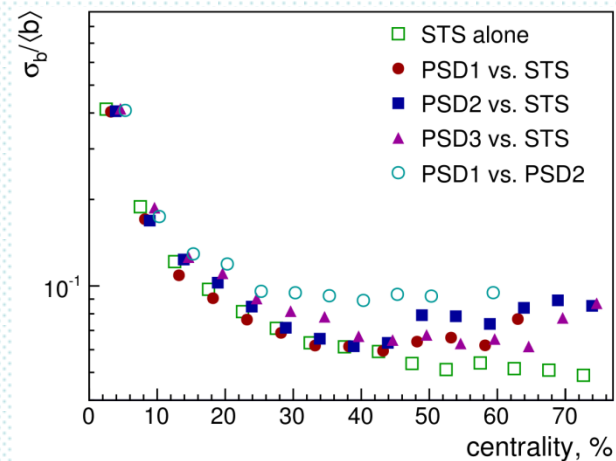


- PSD can be used standalone as an independent centrality estimator with a resolution for centrality of 10%
- PSD helps to improve resolution of the STS for (mid-) central collisions

Average impact parameter, b

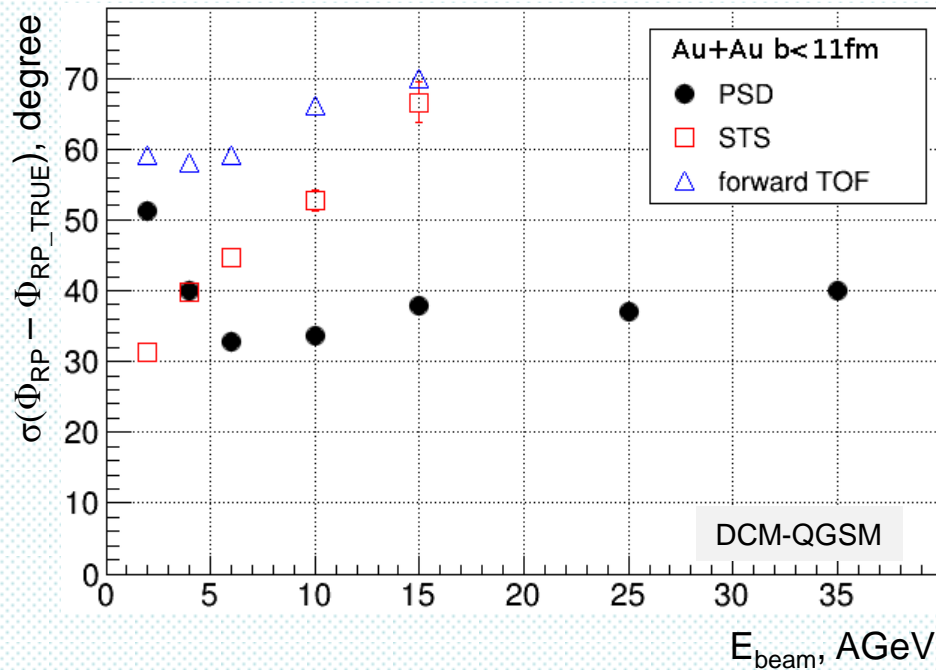


Relative width (\sim centrality resolution)

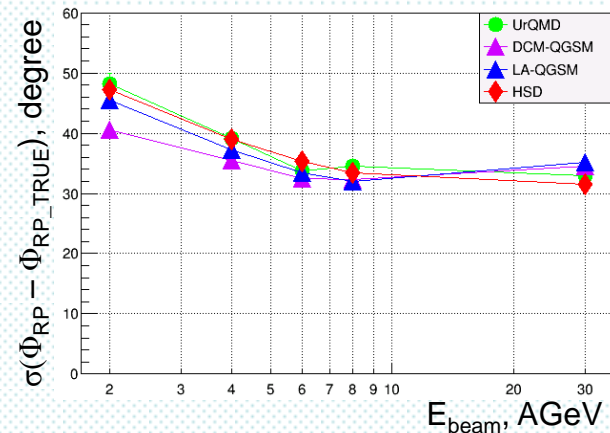
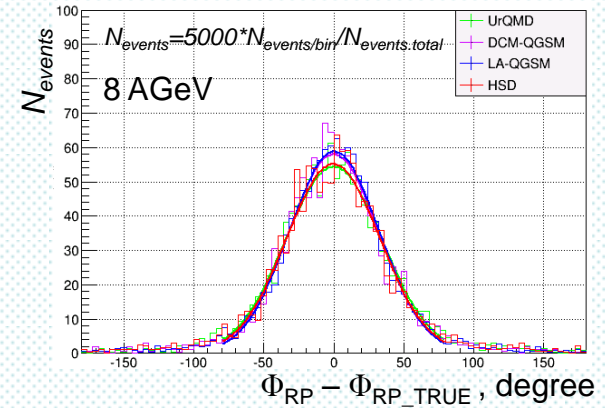


CBM PSD: Reaction plane performance

Reaction plane resolution, σ



Reaction plane resolution



- PSD significantly improves the resolution at energies higher than 4 AGeV.
- Collision event plane resolution is sufficient for precision measurements of directed (v_1) and elliptic (v_2) flow with CBM after a few months of operation

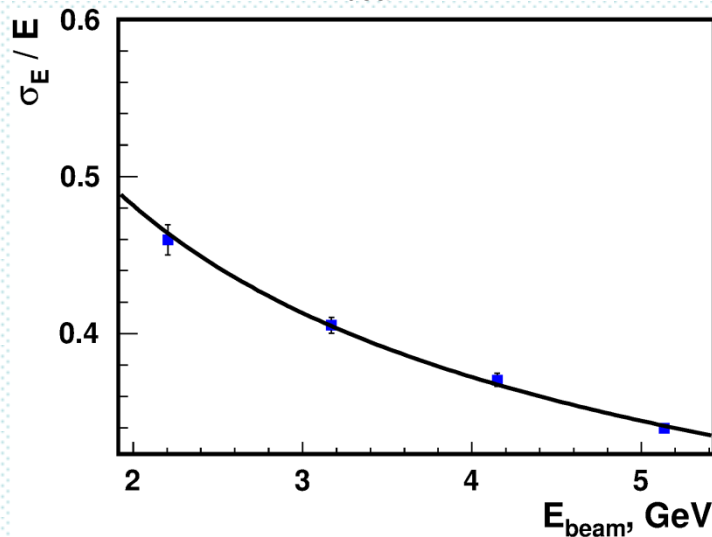
Does σ_{RP} depend on event generator?
 See our poster at Heavy Ion
 Physics Session

CBM PSD: Testing module components

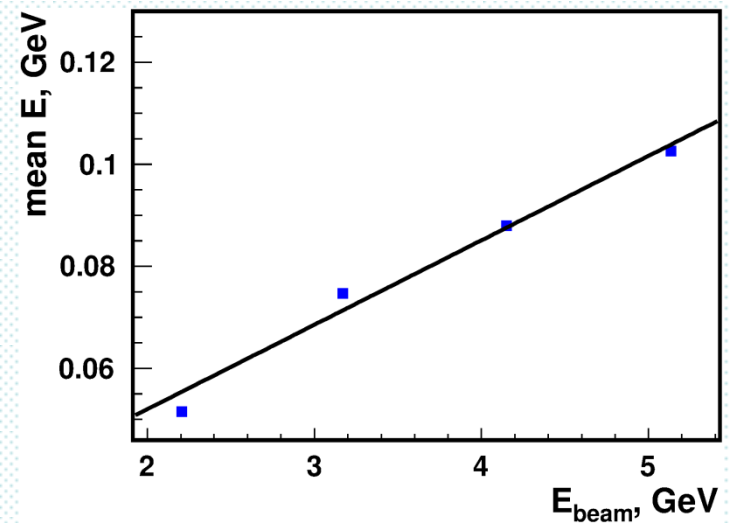
Tested energy resolution, linearity of the response, longitudinal shower profile, and compensation parameters with a 3x3 supermodule at CERN SPS&PS with muon, proton, and pion beams (contaminated by positrons)



Energy resolution with protons $E_{\text{beam}} = 2-6$ GeV



Response linearity



Ongoing:

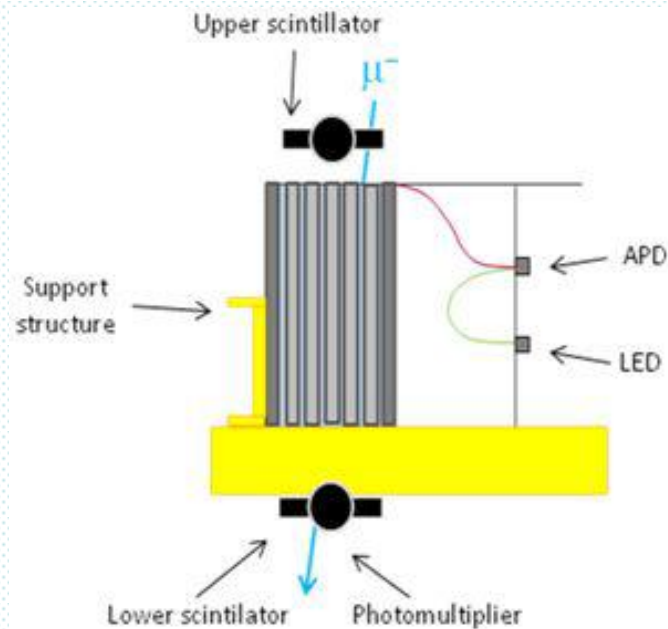
- PSD temperature stabilization system
- Mechanical support
- APD radiation hardness investigation

CBM PSD: APD radiation hardness

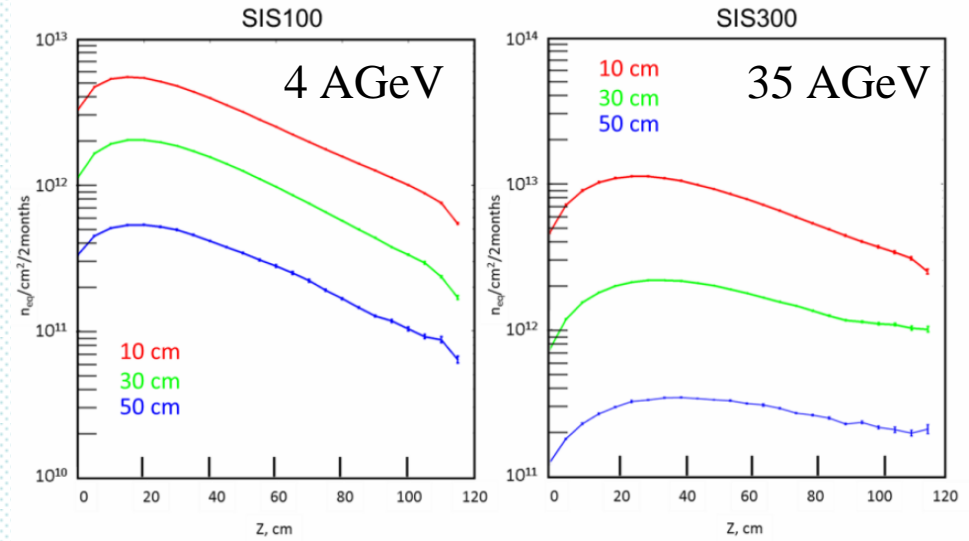
The most critical effect:

the Avalanche photodiodes' (APDs) degradation caused by the neutron flux through the rear side of PSD calorimeter.

Scintillators and other parts are not expected to be much damaged.



Setup for the APDs tests with cosmic muons and LED.



Distributions of the neutron flux ($n/cm^2/s$) through the PSD calorimeter at radius 10, 30 and 50 cm

FLUKA simulation results:

Flux near the beam hole after 2 months of CBM run at the beam rate 10^8 ions/s:

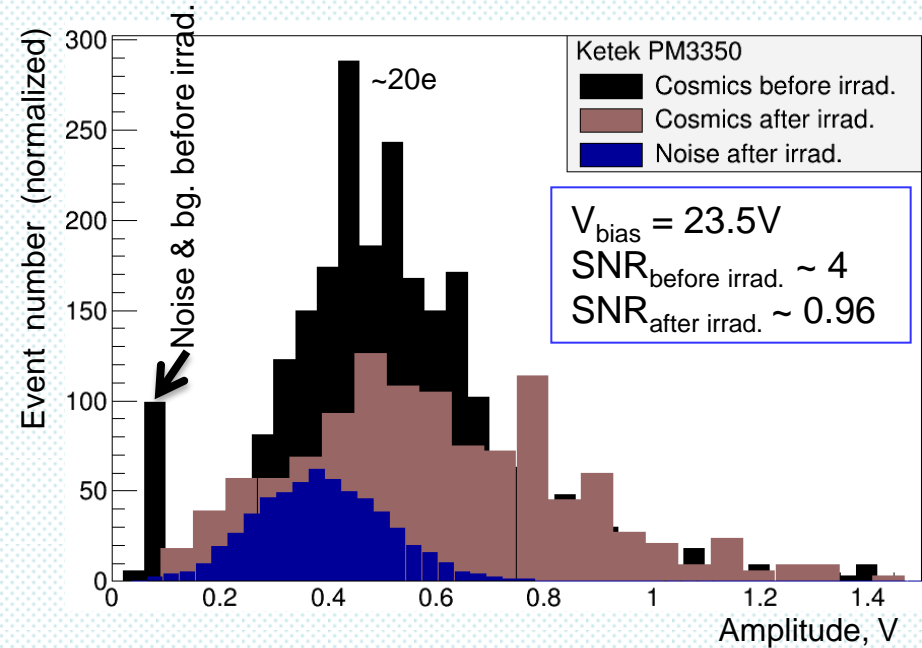
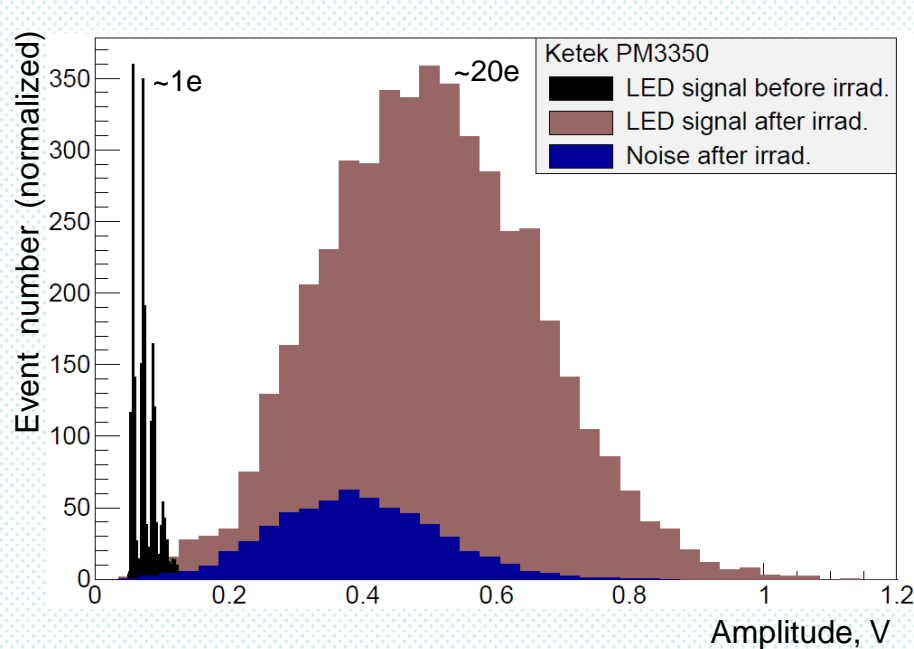
10^{12} n/cm^2 for $E_{\text{beam(Au)}}$ 4 AGeV

4×10^{12} n/cm^2 for $E_{\text{beam(Au)}}$ 35 AGeV

CBM PSD: APD radiation hardness

APD tests with light emitting diode and cosmic muons

Ketek PM3350, Flux of $2.5 \pm 0.2 \times 10^{12}$ n/cm²



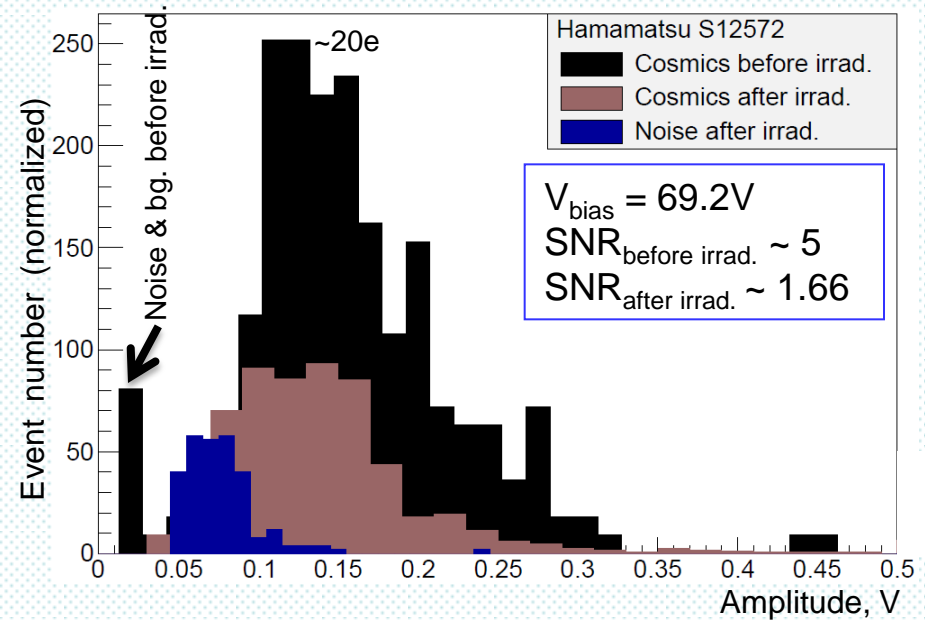
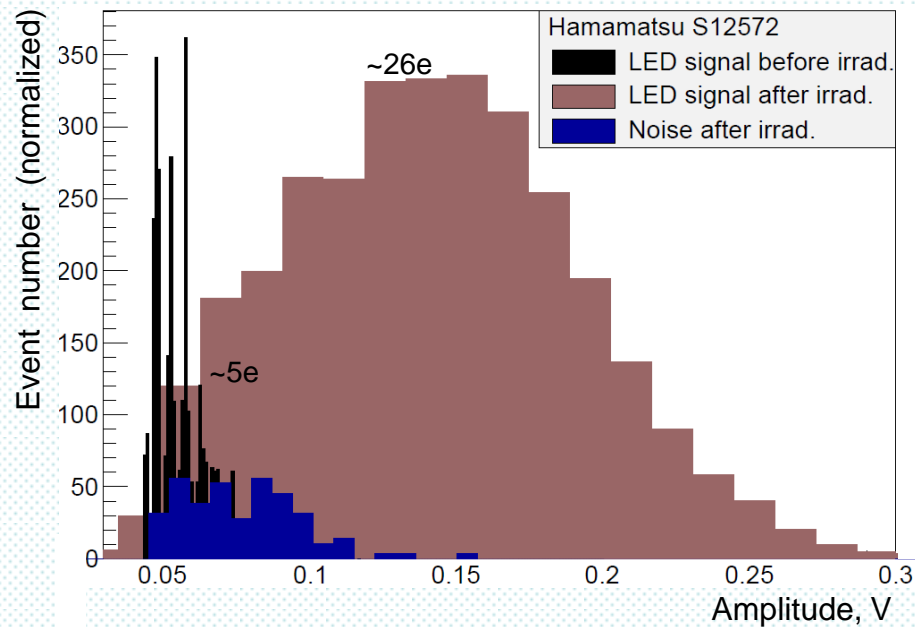
- The irradiation increases the APDs internal noise substantially what leads to inability to detect single photons.
- Signal and noise corresponding to cosmic peaks are overlapping.
- These studies are important for development and upgrades of all mentioned calorimeters.

Irradiated by 35 MeV secondary neutron beam with white spectrum from Cyclotron of NPI at: 7.10.2013, 21.11.2014, 25.06.2015
Dose was recalculated to 1MeV neutrons
During measurements $T = 22 \pm 0.5$ °C

CBM PSD: APD radiation hardness

APD tests with light emitting diode and cosmics muons

Hamamatsu S12572-010P, Flux of $6.5 \pm 0.6 \times 10^{10}$ n/cm²



- The irradiation increases the APDs internal noise substantially what leads to inability to detect single photons.
- Signal and noise peaks corresponding to cosmics are well separated.
- It will be investigated further with flux $\sim 10^{12}$ n/cm²

More advanced techniques like dark current measurement, C-V and C-F profiling were applied!

See our poster at Detector R&D and Data Handling Session

SUMMARY

- **Hadron Calorimeters are important part of experiments of high energy physics for the measurement the energy of non-interacting nucleons and fragments.**
- **Hadron Calorimeters are used for the collision's centrality and reaction plane determination.**
- **R&D on Hadron Calorimeters is a viable task nowadays.**

OUTLOOK

Investigation of Avalanche Photodiodes radiation hardness is ongoing:

- APDs from Sensl MicroFC-30020 and MicroFB-30020 are being tested.**
- APDs from Excelitas C30742-33 are planned to be tested.**
- Advanced investigation techniques are being applied and analyzed.**

Thank you for attention!

Nuclear Research Institute AS CR, Řež

V. Mikhaylov for EPS-HEP 22-29 July 2015

Backup:

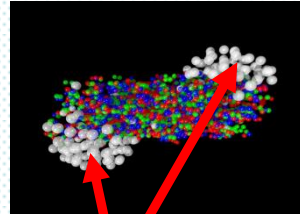
CBM PSD Performance

(from talk of I. Selyuzhenkov at DPG2015)

Centrality determination

Number of interacting participants:

$$N_p = A - \frac{E_s}{E_a}$$



A – mass number of ion

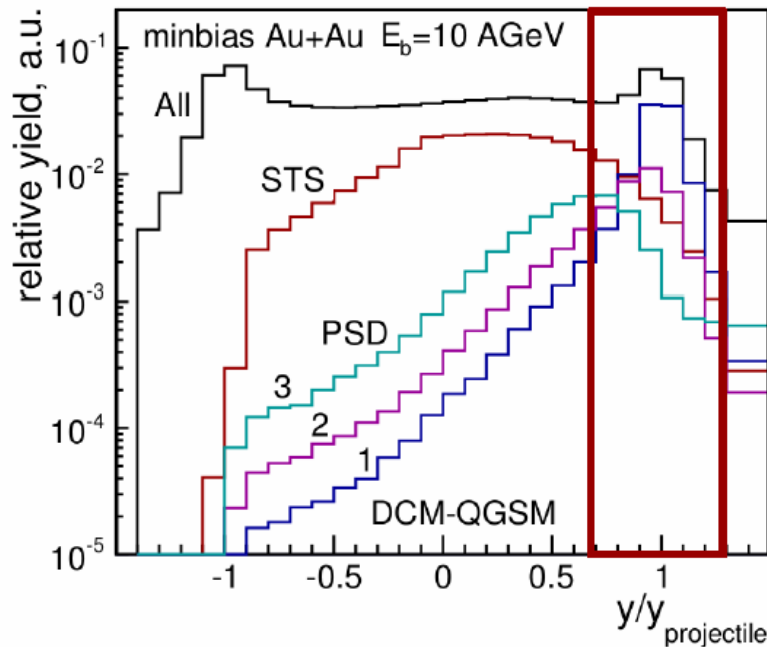
E_a – beam energy per nucleon

E_s – energy carried by the non-interacting nucleons (projectile spectators) -

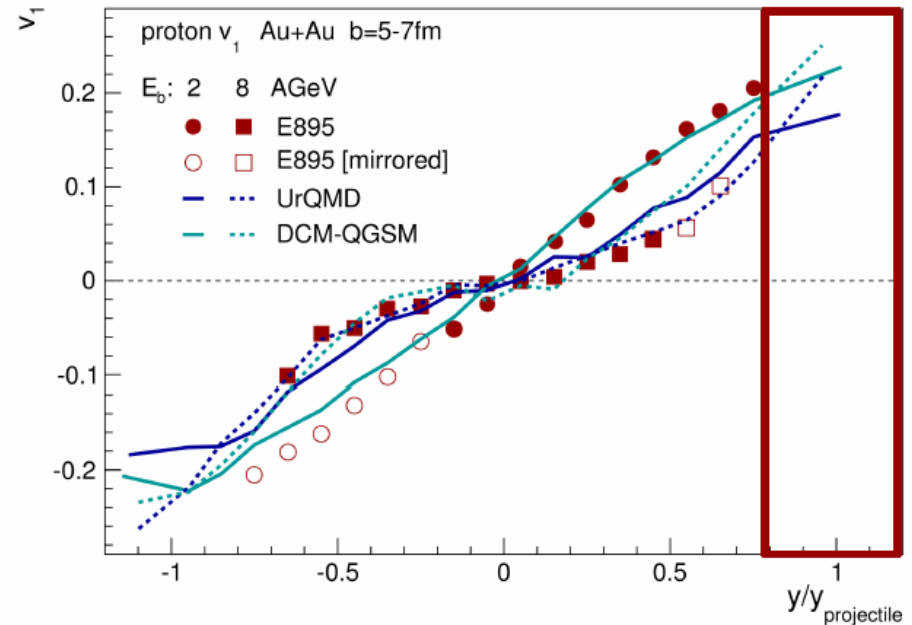
- measured by Hadron Calorimeter

Why spectators are relevant for event geometry determination in CBM?

yields of participants & spectators



directed (v_1) flow

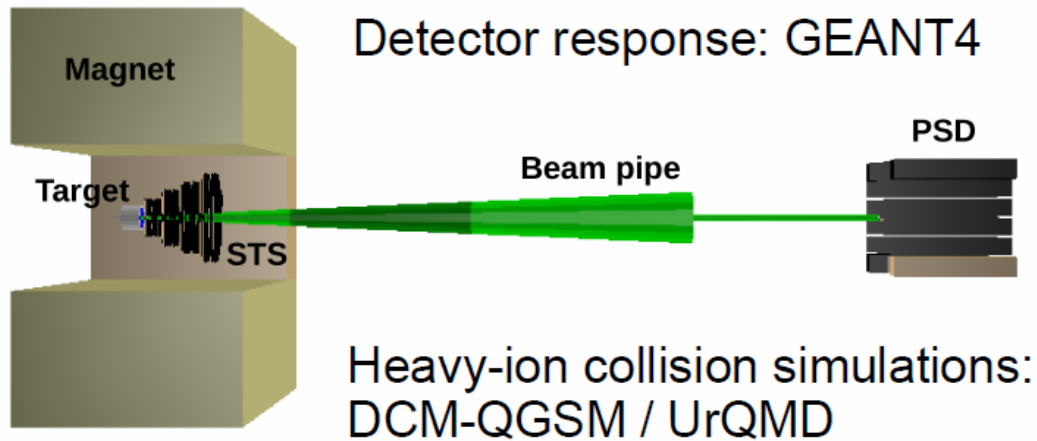


Forward (spectator) region is well suited for collision geometry determination:

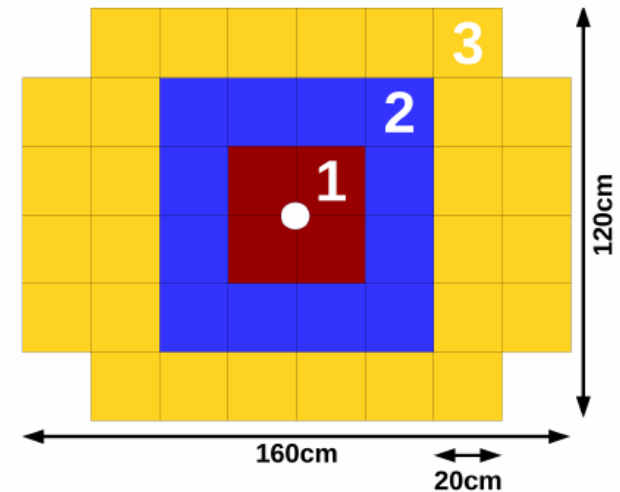
- Provide an independent method to determine centrality
→ important to validate the “participant” centrality estimates at midrapidity
- Strong v_1 (compared to weak v_1 seen by midrapidity detectors of CBM)
→ better reaction plane resolution

Simulation setup for physics performance study

Simulation setup



Transverse geometry



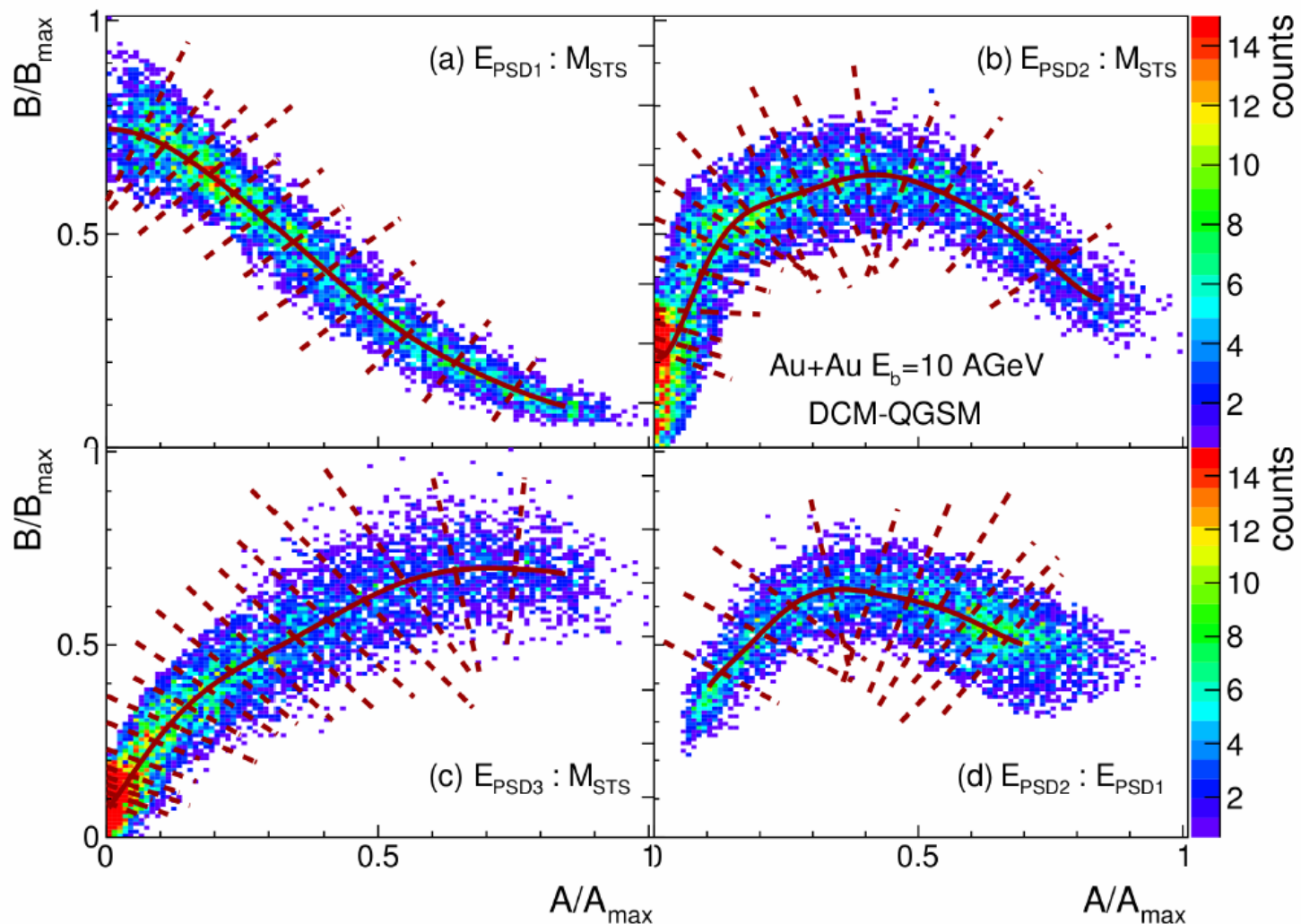
Elongated geometry accounts for smearing of charge fragment distribution along the x-axis by the CBM Magnet:

- Important for azimuthal asymmetry measurements such as anisotropic flow / reaction plane reconstruction

Using subevents:

- allows to use the PSD detector standalone for both centrality and event plane resolution determination
- in a combination with an STS tracking sub-detector helps to improve the overall centrality resolution in CBM

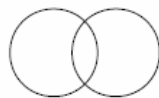
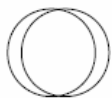
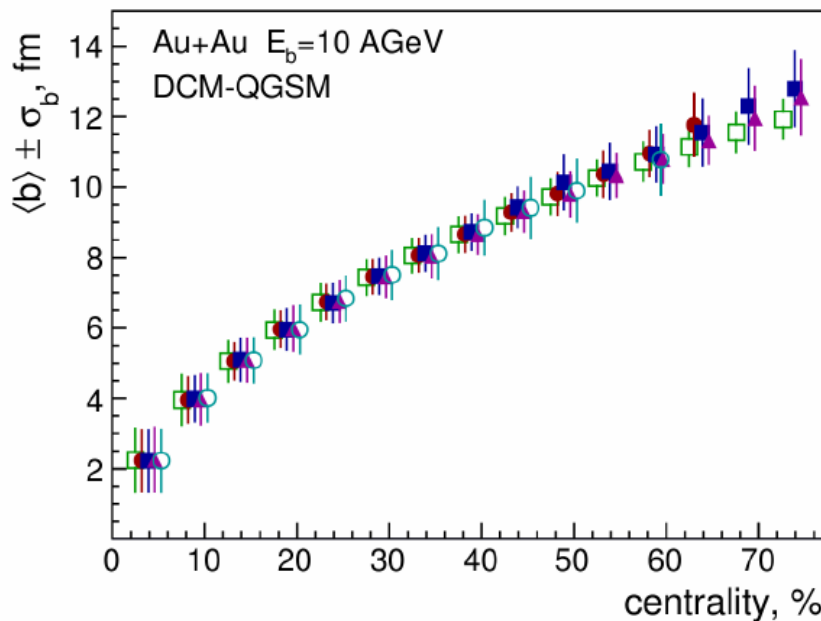
Centrality determination in CBM: Correlation between PSD subevents & STS track multiplicity



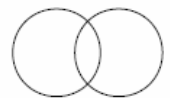
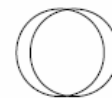
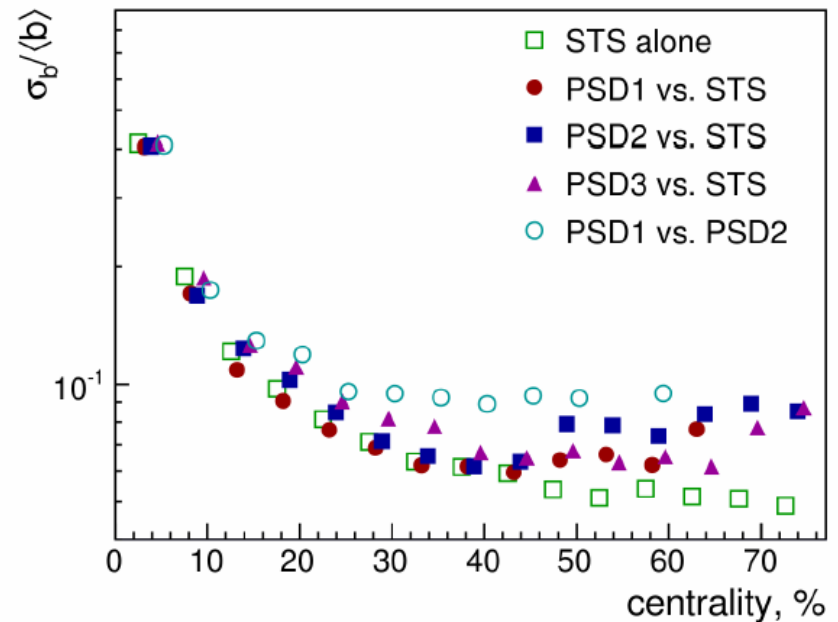
Two (mutli)-dimensional correlations of energy deposited in PSD subevents can be used to define centrality classes

Centrality determination

Average impact parameter, b



relative width (\sim centrality resolution)



- PSD can be used standalone as an independent centrality estimator with a resolution for centrality of 10%
- PSD helps to improve resolution of the STS for (mid-)central collisions

Anisotropic flow measurement techniques

$$\frac{dN}{d(\varphi_i - \Psi_n)} \sim 1 + 2 \sum_{n=1} v_n \cos[n(\varphi_i - \Psi_n)]$$

$v_n = \langle \cos[n(\varphi_i - \Psi_n)] \rangle$ - directly calculable only in theory when the collision symmetry plane orientation is known

Experimental estimate of the collision symmetry plane based on the measured azimuthal distribution of particles (event plane angle):

$$\Psi_n \rightarrow \Psi_{n,EP} \longrightarrow v_n\{\text{EP}\} = \frac{\langle \cos[n(\varphi_i - \Psi_{EP}^n)] \rangle}{R_n}$$

R_n - event plane resolution correction factor

Using PSD, the event plane angle is defined by center of gravity shift of spectator transverse energy distribution deposited in the PSD (Q - vector):

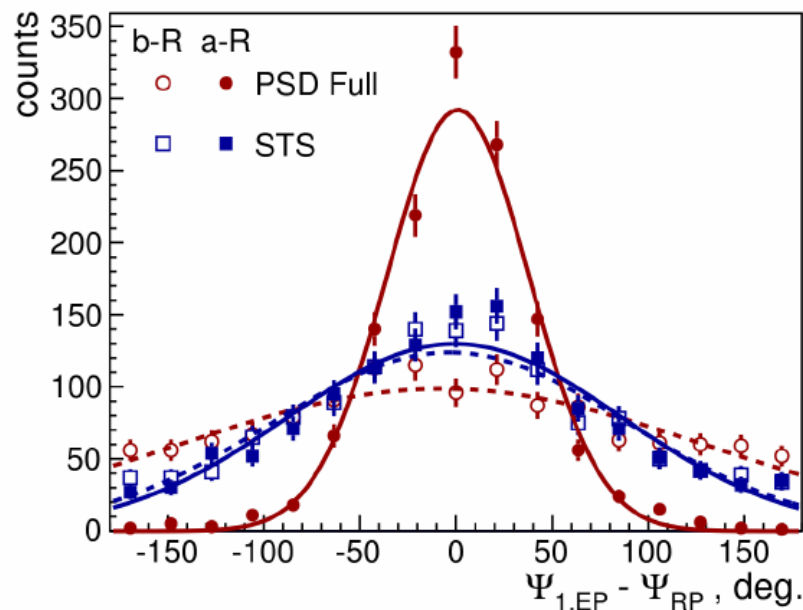
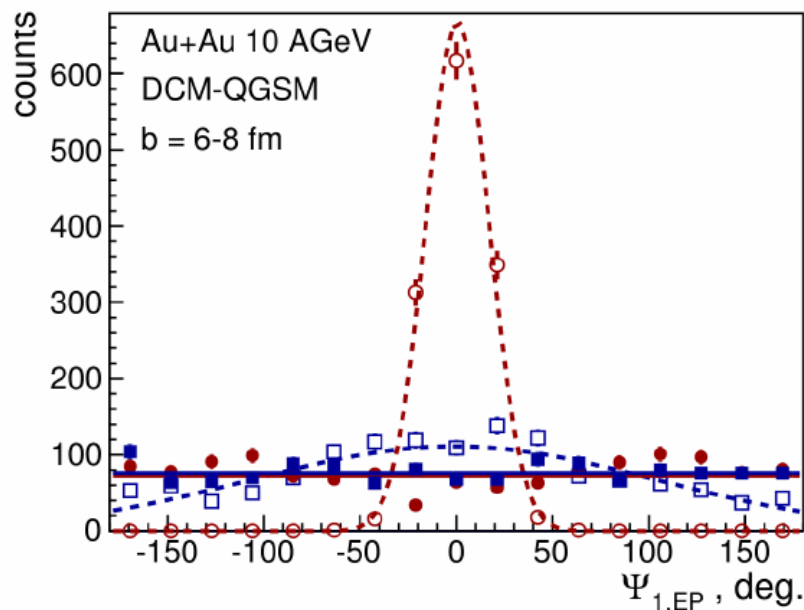
$$Q = (Q_x, Q_y) = \sum_i w_i (\cos \varphi_i, \sin \varphi_i) \quad \Psi_{1,EP} = \text{atan} 2(Q_y, Q_x)$$

Detector corrections for azimuthal non-uniformity

Q-vector recentering:
$$Q_{x,y} = \frac{Q_{x,y} - \langle Q_{x,y} \rangle}{\langle Q_{x,y} \rangle}$$

Event plane distribution before and after recentering

Event plane resolution before and after recentering

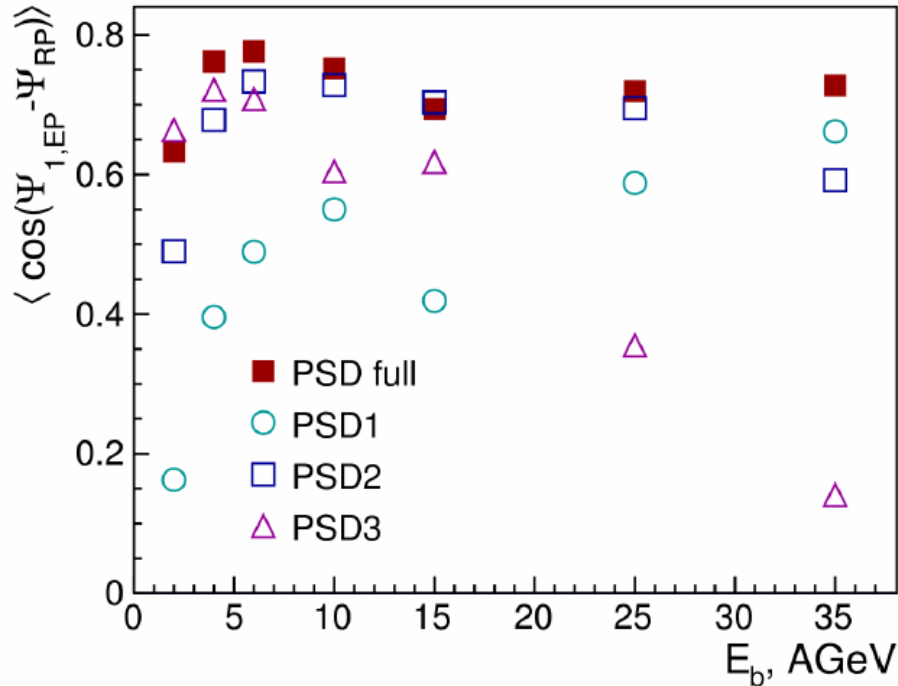


After corrections:

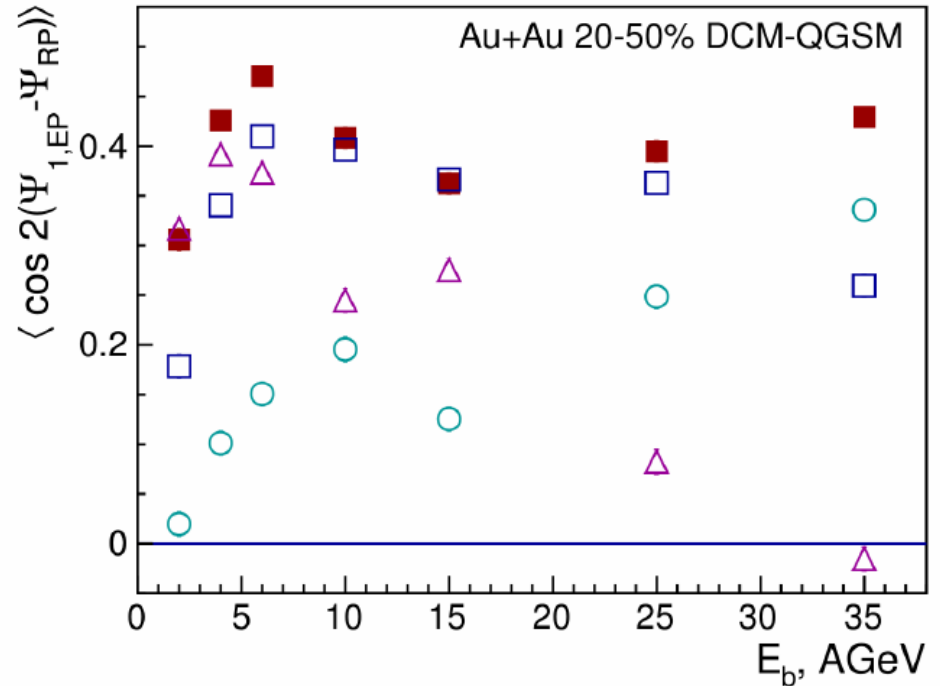
- PSD and STS event plane distributions are flattened
- PSD event plane resolution is improved and better than from STS

Event plane resolution (correction factor)

Correction for directed flow (v_1)



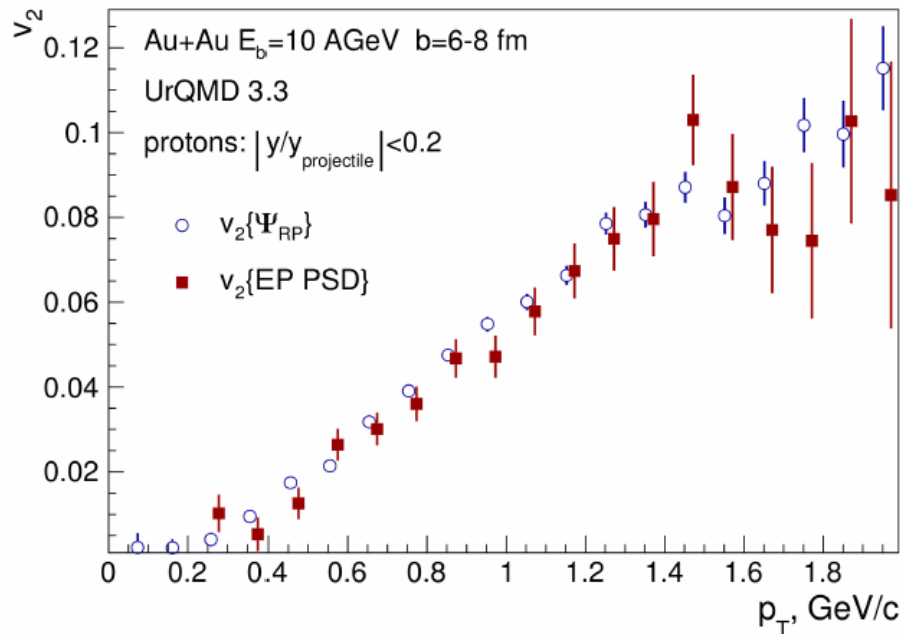
Correction for elliptic flow (v_2)



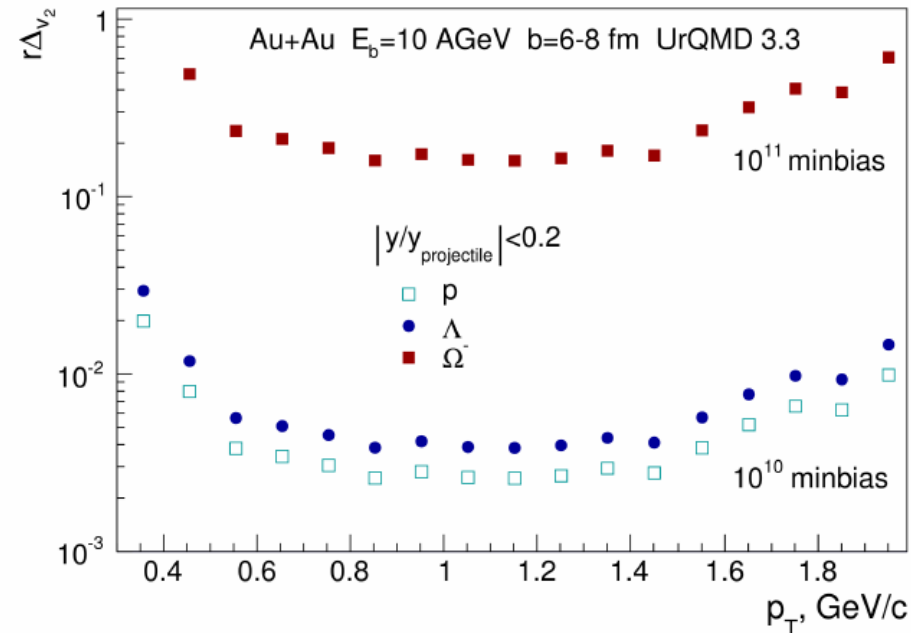
- Sensitivity of different PSD sub-events changes with collision energy
- 1st order event plane distribution is high (0.7-0.8 which is close to ideal case “1”)
- 2nd order event plane resolution with PSD is good (~0.4)

PSD performance for elliptic flow (v_2) measurements

Reconstructed proton v_2 with
PSD event plane correction
from three PSD subevents



Statistical error projections for
(strange-)baryons v_2 after 2 months of
operation at 100kHz interaction rate



- “input” model v_2 is recovered using “data-driven” method with 3 PSD subevents
- Statistical error projections promises high precision measurements of (strange-)baryons v_2 in a wide p_T range between 0.3 - 2.0 GeV/c at mid-rapidity already after 2 months of CBM experiment operation

Summary

- Performance study of the Projectile Spectator Detector (PSD) for CBM is presented
- Detector design relies on a well known technology and materials, which are tested with PSD module prototypes and a similar detector in operation at CERN SPS
- “Physics performance” of the PSD design is demonstrated with a sample of heavy-ion collisions generated with DCM-QGSM and UrQMD models and simulated PSD/CBM response with Monte-Carlo GEANT package:
 - ~10% resolution for collision centrality with PSD standalone configuration provides independent (& unique) way of centrality determination via spectators
 - Collision event plane resolution is sufficient for precision measurements of directed (v_1) and elliptic (v_2) flow with CBM after a few months of operation
- The PSD Technical Design Report (TDR) was approved by FAIR on Feb 26, 2015

Backup:

APD Radiation Hardness

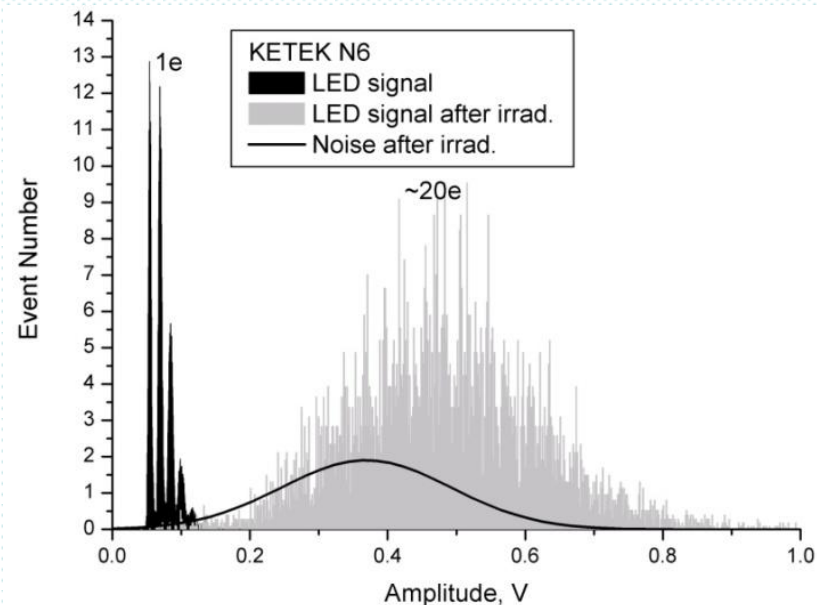
(from talk of V. Kushpil at CBM coll.meet.2015)

CBM PSD: APD radiation hardness

APD tests with light emitting diode

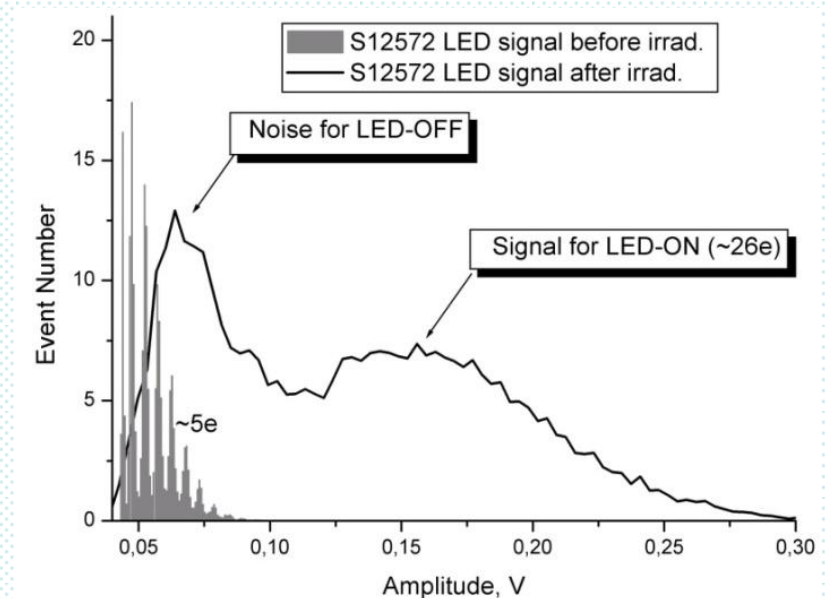
Ketek PM3350

Flux of $2.5 \pm 0.2 \times 10^{12}$ n/cm²



Hamamatsu S12572-010P

Flux of $6.5 \pm 0.6 \times 10^{10}$ n/cm²



Ketek: signal and noise peaks are overlapping.
Hamamatsu: signal and noise peaks are well separated.

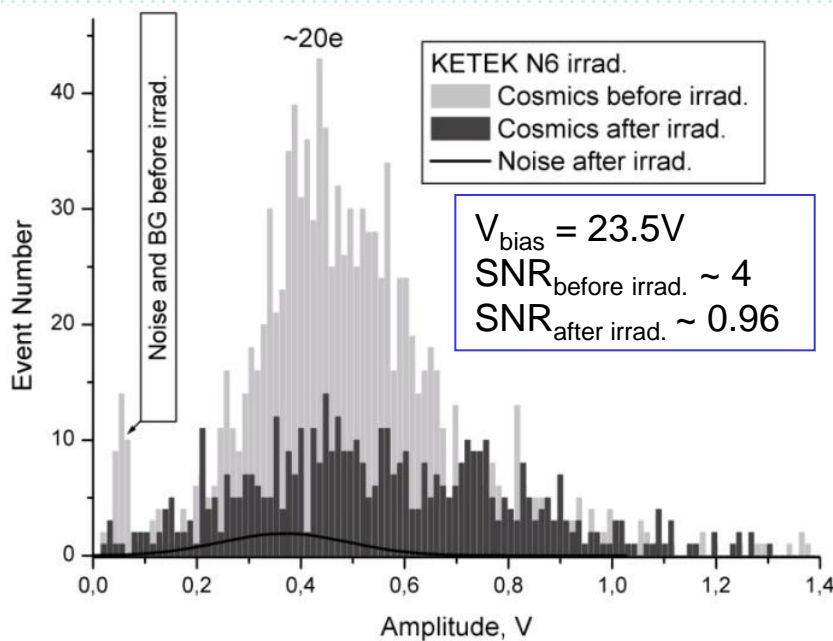
Irradiated by 35 MeV secondary neutron beam with white spectrum from Cyclotron of NPI at:
7.10.2013, 21.11.2014, 25.06.2015
Dose was recalculated to 1MeV neutrons
During measurements $T = 22 \pm 0.5$ °C

CBM PSD: APD radiation hardness

APD tests with cosmic muons

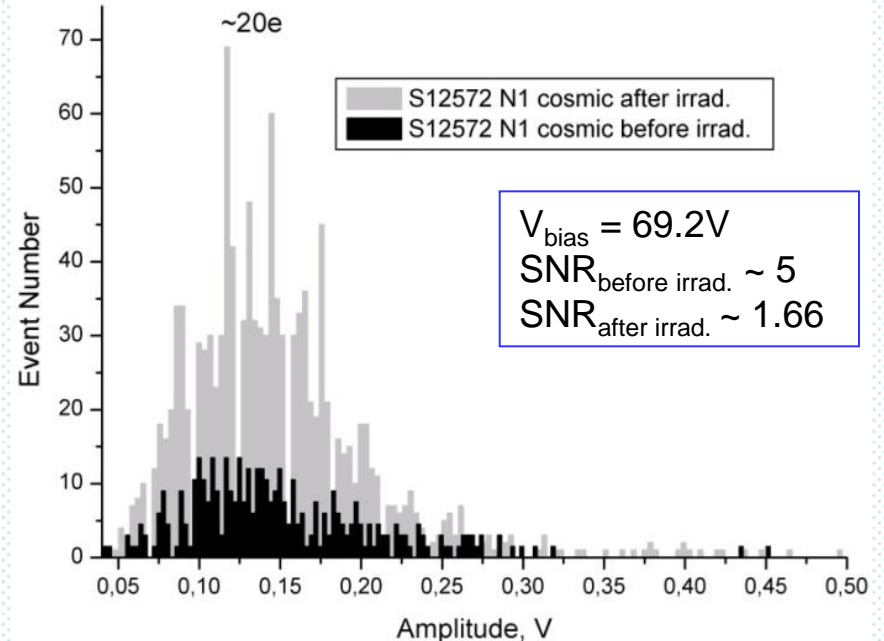
Ketek PM3350

Flux of $2.5 \pm 0.2 \times 10^{12}$ n/cm²



Hamamatsu S12572-010P

Flux of $6.5 \pm 0.6 \times 10^{10}$ n/cm²



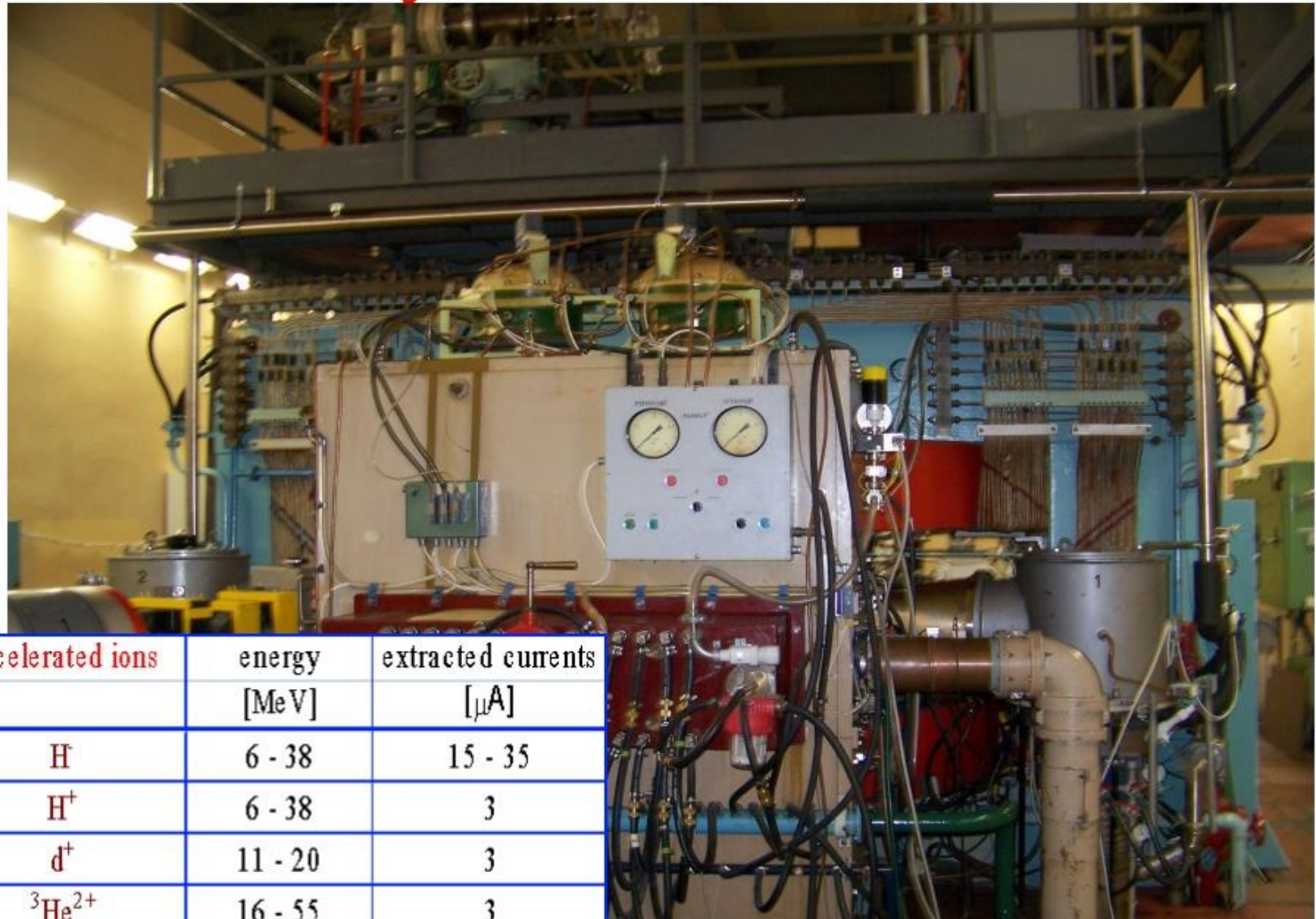
The irradiation increases the APDs internal noise what leads to inability to detect single photons.

These studies are important for development and upgrades of all mentioned calorimeters.

More advanced techniques like dark current measurement, C-V and C-F profiling were applied!

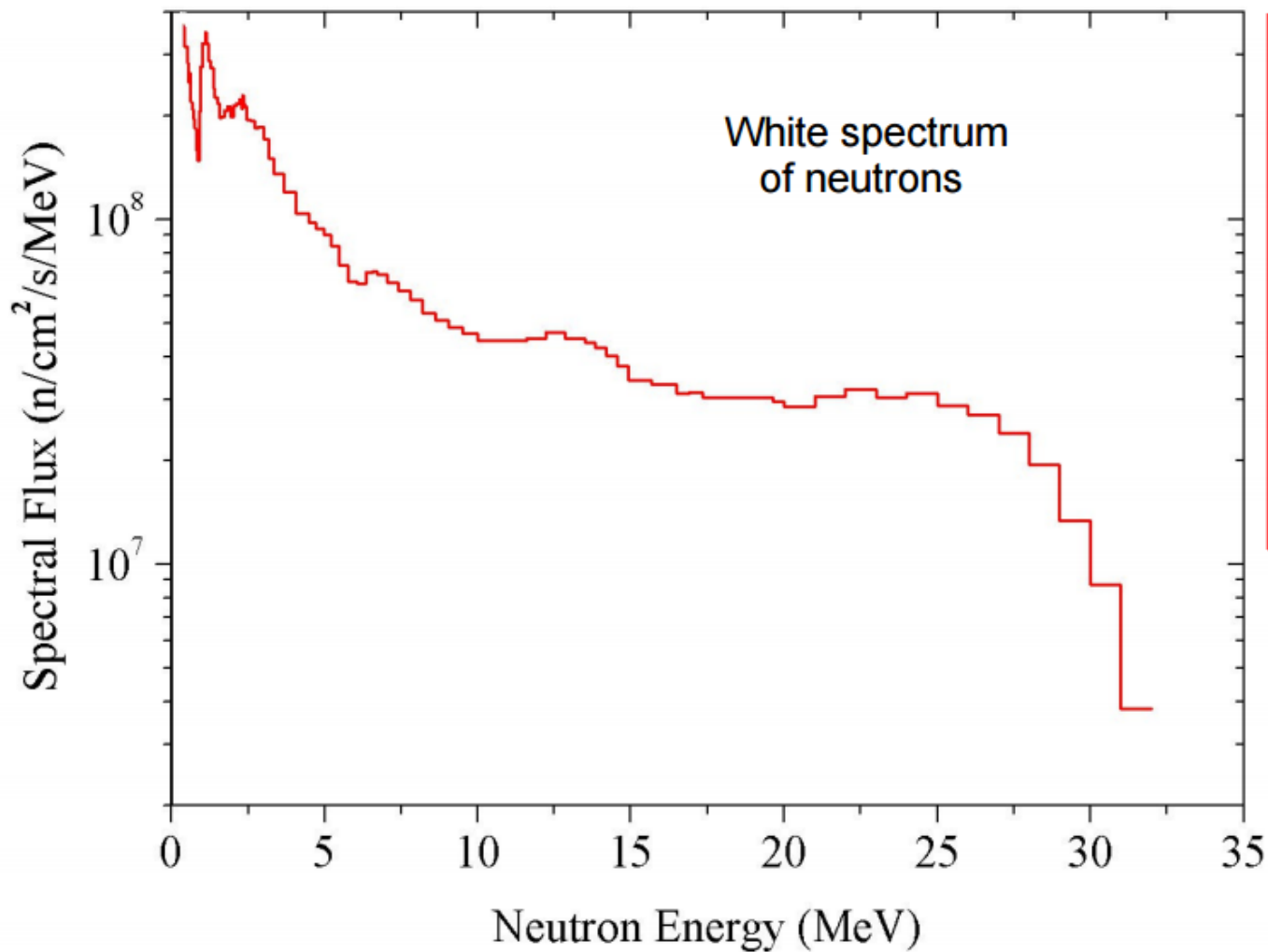
See our poster at *Detector R&D and Data Handling Session*

Cyclotron U120M



accelerated ions	energy [MeV]	extracted currents [μA]
H	6 - 38	15 - 35
H ⁺	6 - 38	3
d ⁺	11 - 20	3
³ He ²⁺	16 - 55	3
⁴ He ²⁺	22 - 40	3

Cyclotron U120M (p + D₂O)



**For source NG1
Maximum of Flux**

**~10⁸ - 10⁹-
[n/cm²/s]**

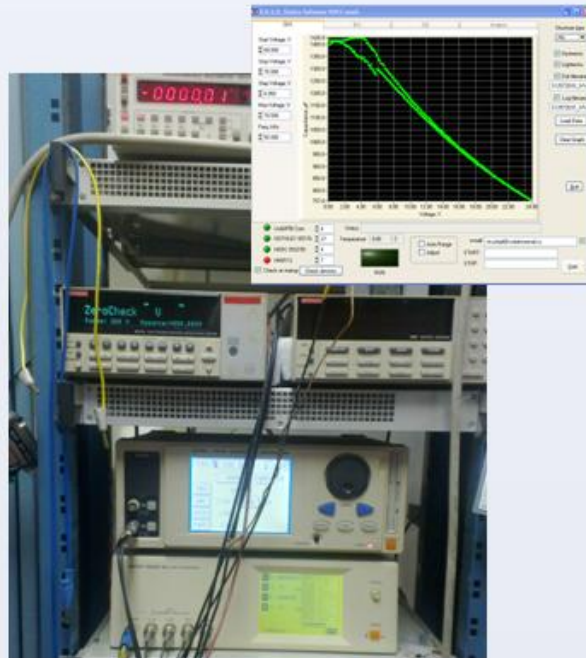
**For source NG2
Maximum of Flux**

~10¹¹ [n/cm²/s]

Methods of APD investigation

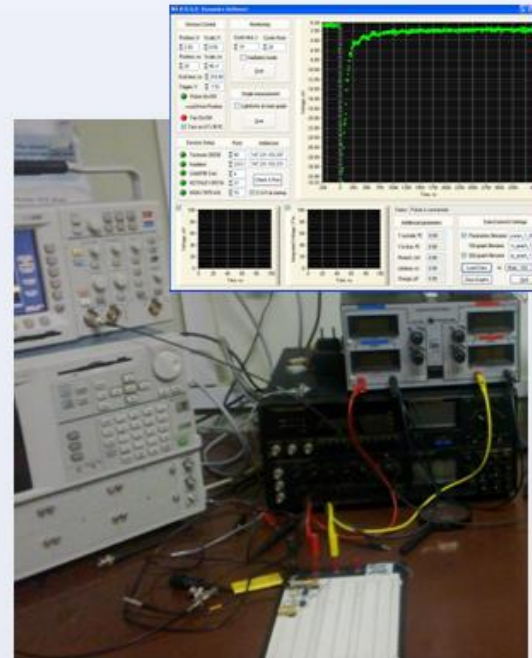
Static characteristics (C-V, C-F, I-V)

- investigation of internal structure of APD
- studying of the behaviors of impurities during APD operation
- measurement of the parameters of APD for equivalent circuit of APD in SPICE



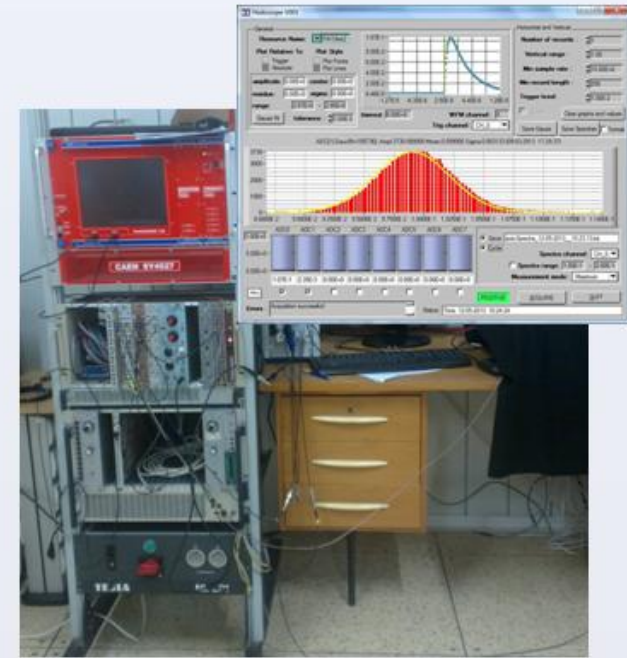
Dynamic characteristics (transient effects)

- investigation of generation and recombination processes into APD bulk
- studying of noise sources behaviors of APD
- measurement of the parameters of noise sources for SPICE model of APD

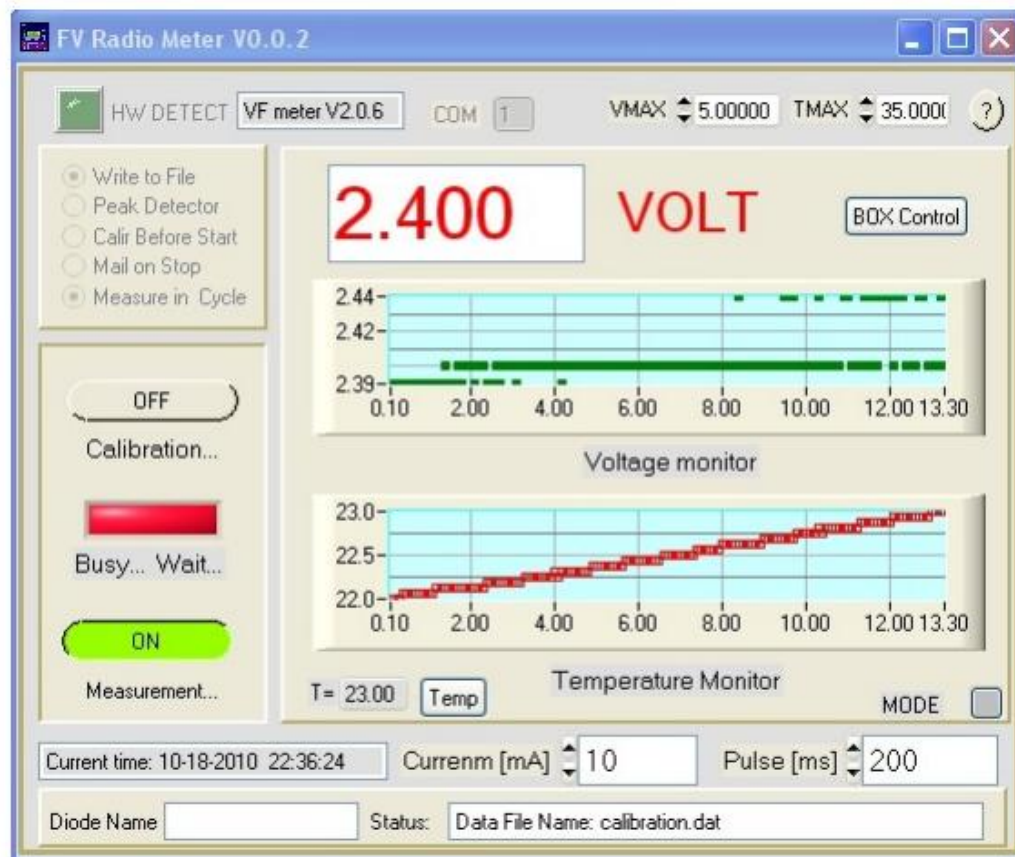
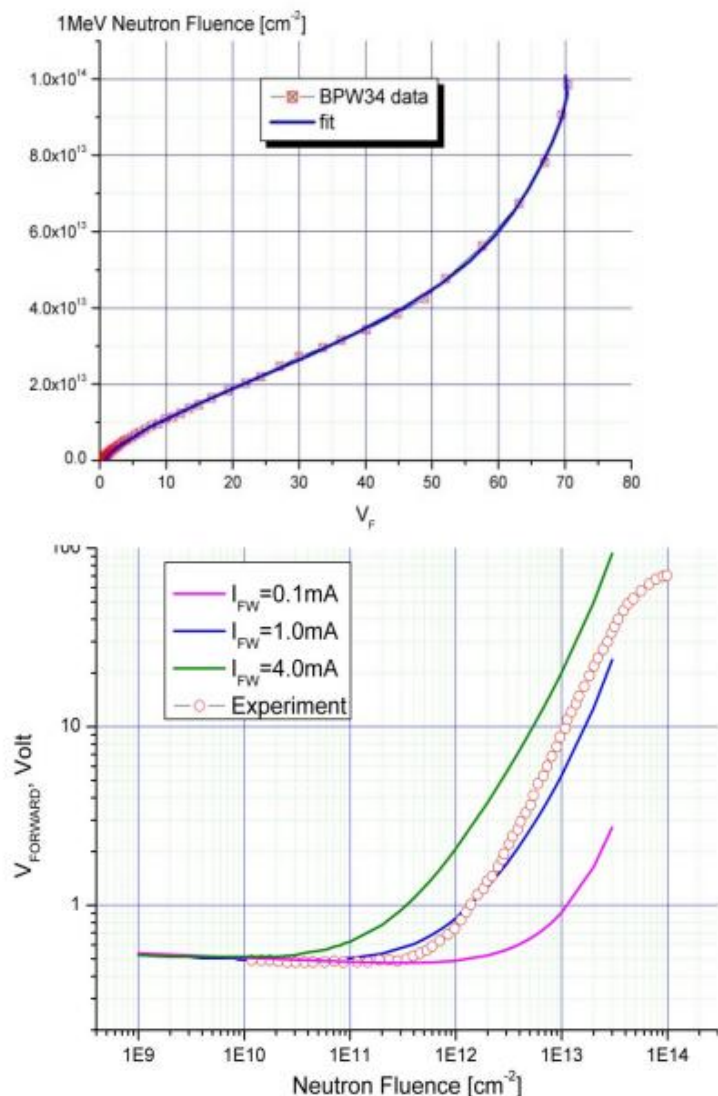


Operation of APD

- single photon spectrum measurement with LED
- investigation of APD with scintillator and radioactive sources in laboratory
- investigation of APD with scintillator for cosmic rays

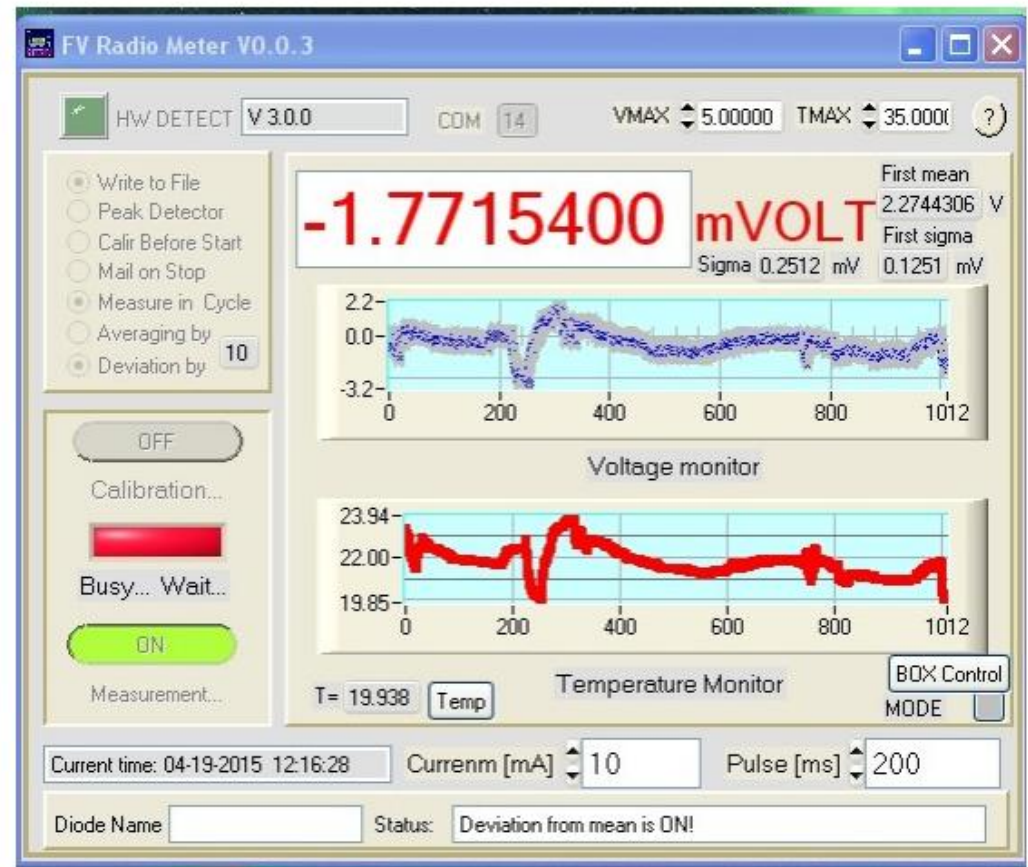
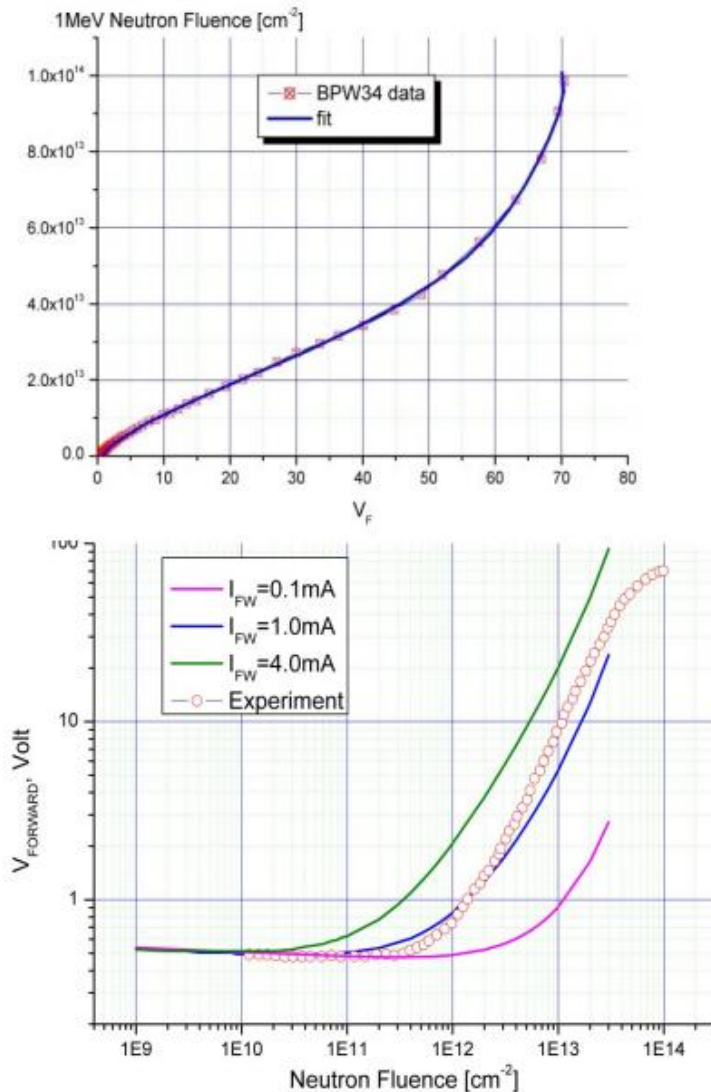


Monitoring of absorbed dose



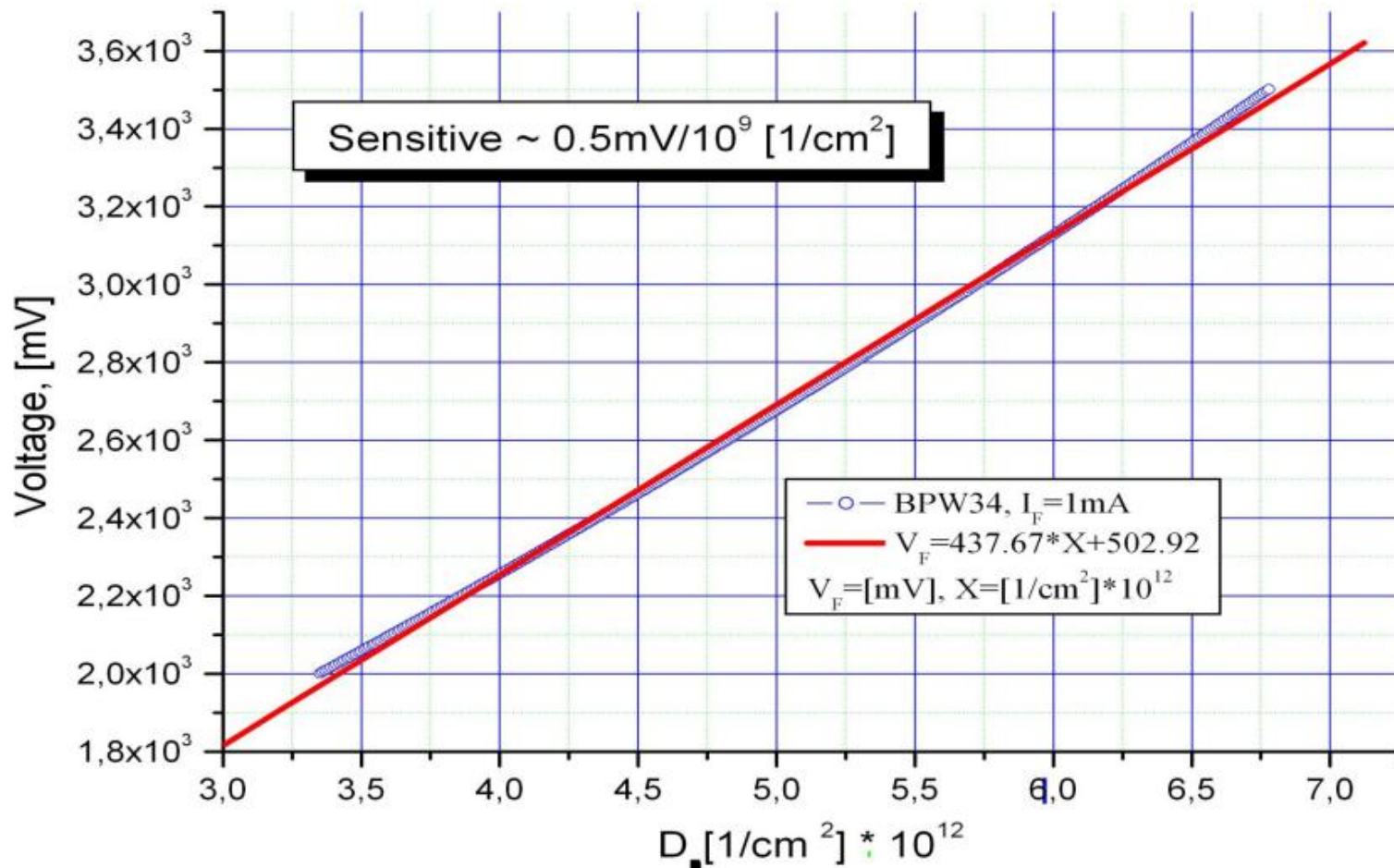
Presented in October 2010 (Rome)
International Conference on Environmental Radioactivity –
New Frontiers and Developments

Monitoring of absorbed dose V003



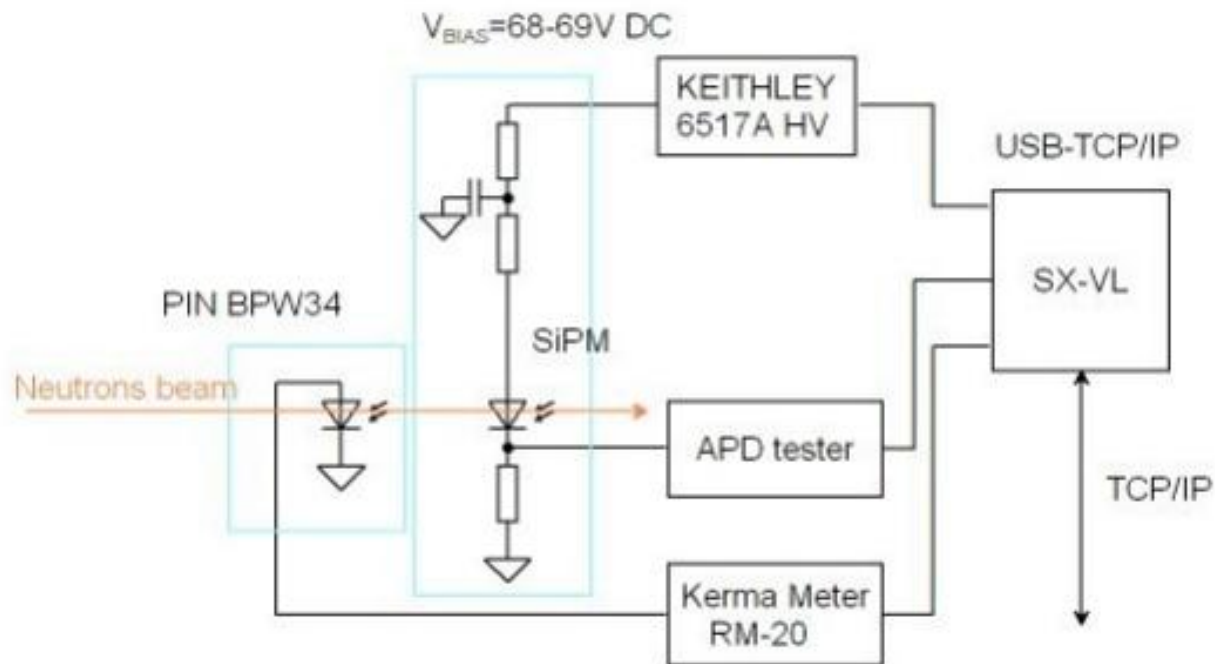
**22bit ADC resolution ~150uV,
before modification ~ 1000uV**

Monitoring of absorbed dose



We will use Improved method of measurement of voltage and expect to reach sensitivity of monitoring $\sim 1\text{mV}/10^9 \text{ n/cm}^2$

Method of Measurement



APD for test

- We investigated:

5 MAPD-3N (ZECOTEK) Gain~10000, 5um/cell;

7 SiPM PM3375 (from 10) Gain~10E⁶, KETEK 50um/cell;

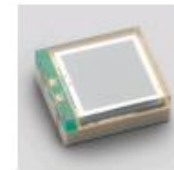
2 MPPC S12572 (from 10) Gain~10E⁶ (HAMAMATSU) 10um/cell;



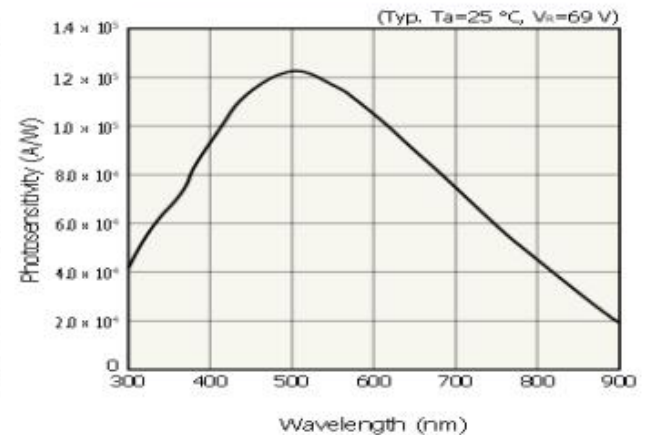
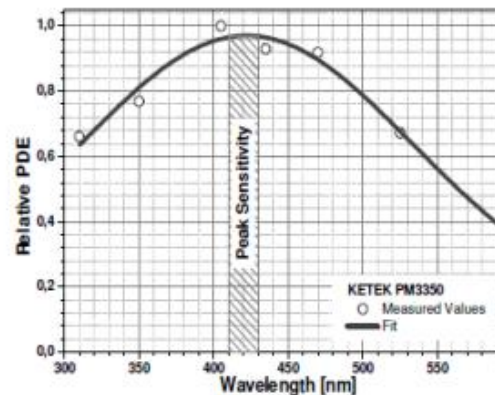
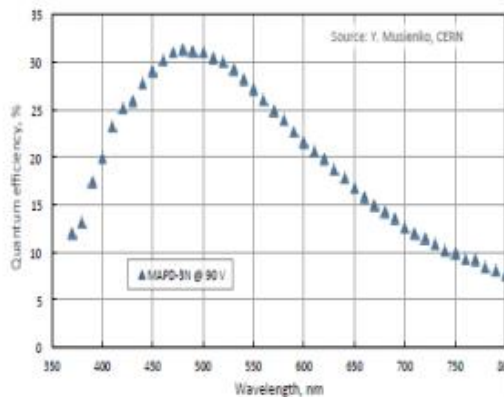
MAPD-3N



PM3375



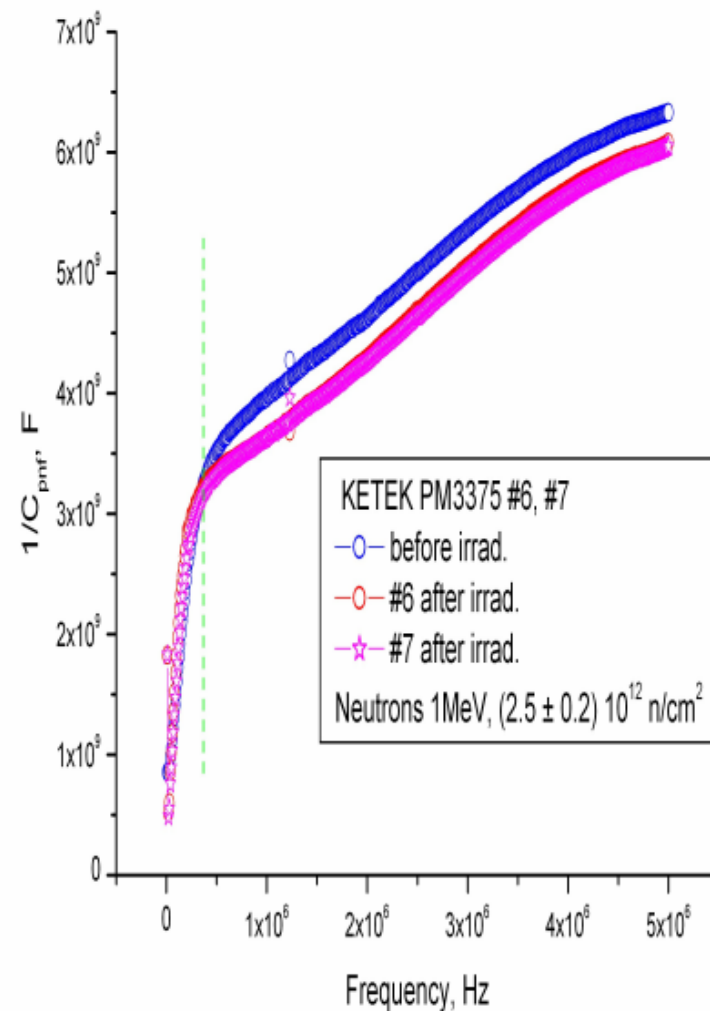
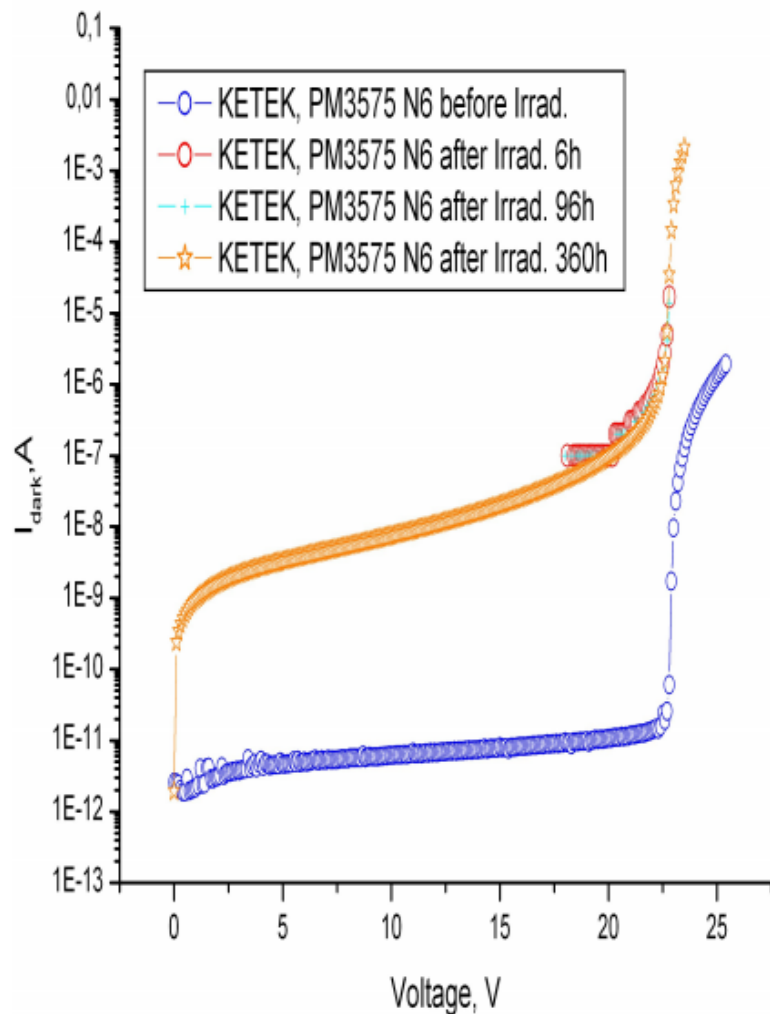
S12572



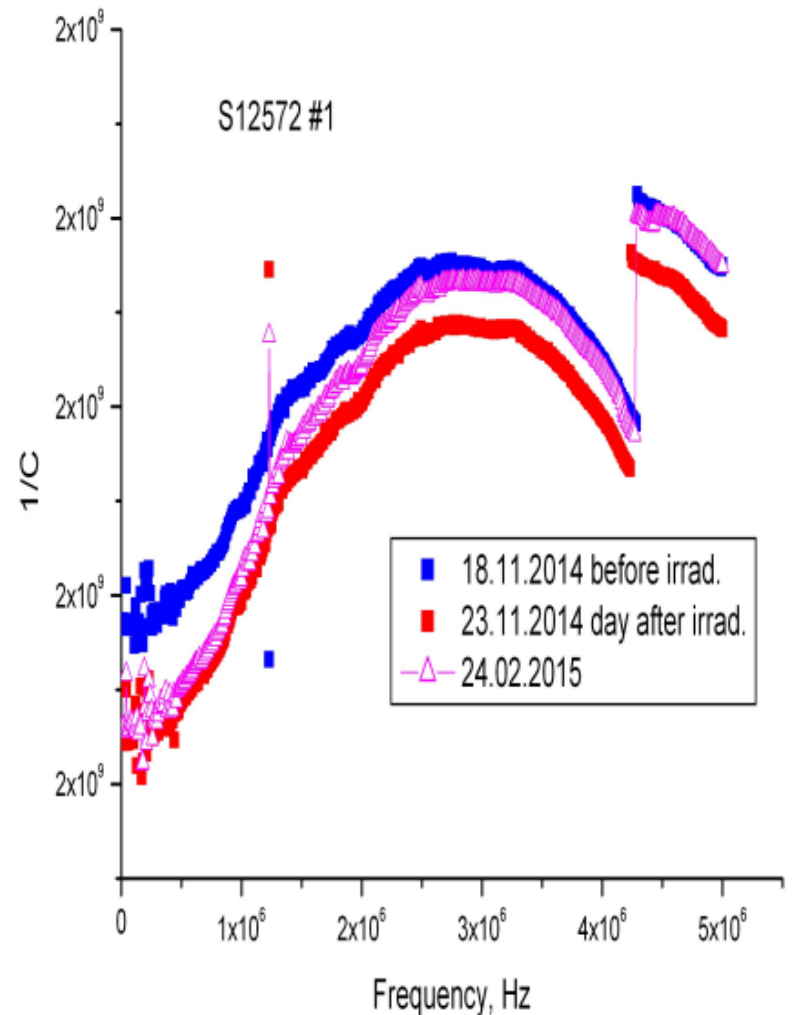
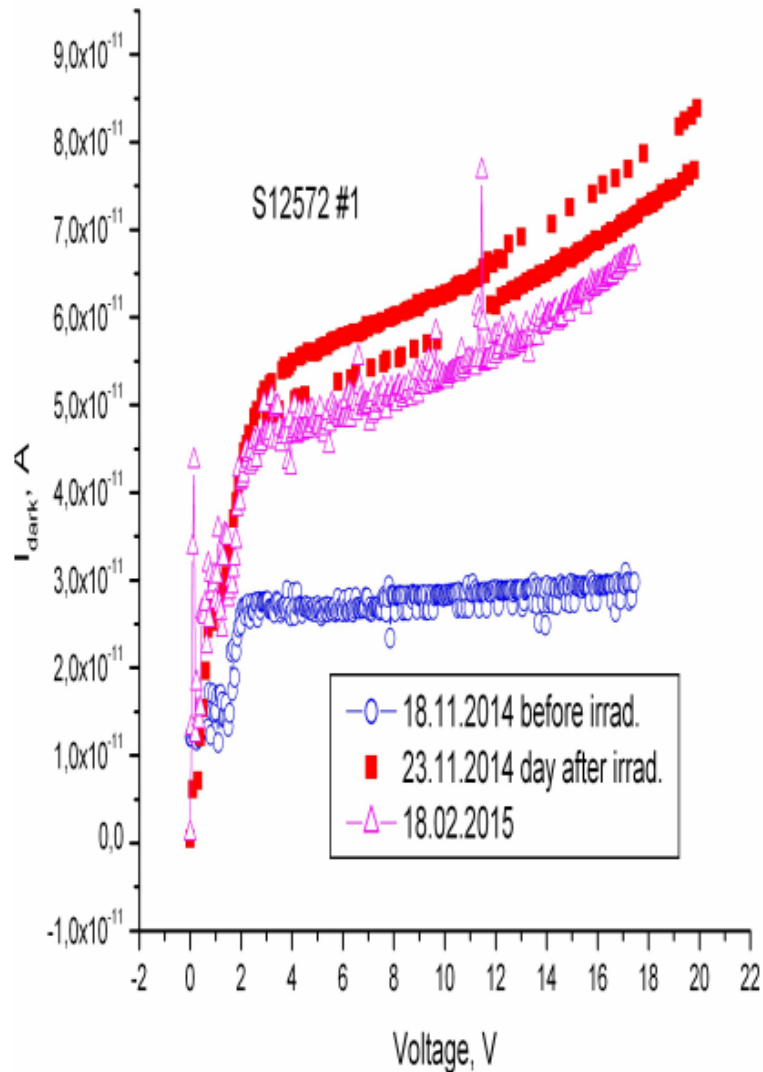
2x APD PM3375 and 1x APD MAPD-3N, 1x APD S12572 were irradiated by neutrons with equivalent dose for 1MeV neutrons:

PM3375	$2.5 \pm 0.2 \cdot 10^{12}$ n/cm ²
MAPD-3N	$3.4 \pm 0.2 \cdot 10^{12}$ n/cm ²
S12572	$6.2 \pm 0.6 \cdot 10^{10}$ n/cm ²

SiPMD KETEK self annealing



HAMAMATSU self annealing



Results

Type	V_{bias}	Fluence	SNR(*) before irr.	SNR(*) After irr.
MAPD-3N	$V_{bias} = 90.2V$	$3.4 \pm 0.2 \cdot 10^{12} [1/cm^2]$	SNR~3	SNR~1.5
PM3375	$V_{bias} = 23.5V$	$2.5 \pm 0.2 \cdot 10^{12} [1/cm^2]$	SNR~4	SNR~0.96
S12572	$V_{bias} = 69.2V$	$6.5 \pm 0.6 \cdot 10^{10} [1/cm^2]$	SNR~5	SNR~1.66

ZECOTEK –
 N_{traps} with $\tau_t > 2.5 \mu s$ decreased
 N_{traps} with $\tau_t < 2.5 \mu s$ increased
 according to $\frac{1}{C_{pnf}}(f) = k \cdot \frac{\tau_t}{N_t} \cdot f$ [5]

KETEK -
 N_{traps} with $\tau_t > 0.5 \mu s$ decreased
 N_{traps} with $\tau_t < 0.5 \mu s$ increased

HAMAMATSU – N_{traps} with $\tau > 0.75 \mu s$ not selfannealing

(*) $SNR \sim \langle S \rangle / \sigma$